QEX

A Forum for Communications Experimenters

November/December 2025
Issue No. 353 | www.arrl.org

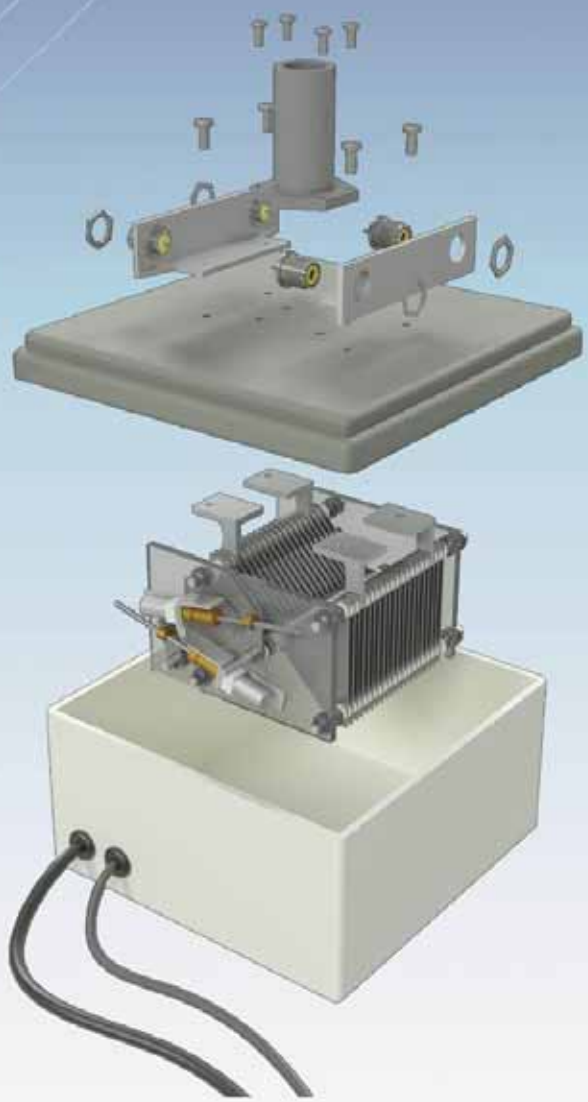

Magnetic loop antenna tuning assembly.

KENWOOD

Versatile and Flexible Radio Returns with a New Look and Soaring Functions That'll Thrill Amateur Radio Enthusiasts.

NEW TRIBANDER

TH-D75A

144 / 220 / 430 MHz TRIBANDER

Key Features

- **APRS® Protocol*1 compliant**
  To exchange GPS location data and messages in real-time.
- **D-STAR*2 with Simultaneous Reception on DV mode**
  Compatible for transferring voice and digital data over D-STAR networks.
- Reflector Terminal mode to access D-STAR Reflectors
- USB Type-C for Data Transfer and Charging
- Built-in Digipeater (a digital repeater) station to transmit received data
- Built-in GPS unit
- Easy-to-read Transflective Color TFT Display
- Call Sign Readout
- Tough & Robust – meets IP54/55 Standards
- Wide-band and multi-mode reception
- Built-in IF Filter for comfortable reception (SSB/CW)
- DSP-based Voice Processing and Reputable KENWOOD Custom Tuned Sound Quality
- Bluetooth®, microSD/SDHC Memory Card Slot for flexible link with a PC

*1: APRS® (The Automatic Packet Reporting System) is a registered trademark of TAPR (Tucson Amateur Packet Radio Corp.)
*2: D-STAR is a digital radio protocol developed by JARL (Japan Amateur Radio League).

JVCKENWOOD USA Corporation

Customer Support/Distribution Customer Support:
(310) 639-4200 Fax: (310) 537-8235 **www.kenwood.com/usa**

ADS#31823

QEX (ISSN: 0886-8093) is published bimonthly in January, March, May, July, September, and November by the American Radio Relay League, 225 Main St., Newington, CT 06111-1400. Periodicals postage paid at Hartford, CT and at additional mailing offices.

POSTMASTER: Send address changes to: QEX, 225 Main St., Newington, CT 06111-1400
Issue No. 353

Publisher
American Radio Relay League

Ronald Diehl, NQ8W
Editor

Lori Weinberg, KB1EIB
Assistant Editor

Publications Department
Becky R. Schoenfeld, W1BXY
Director of Publications and Editorial

Matt Ali
Layout & Production Specialist

David Pingree, N1NAS
Senior Technical Illustrator

Brian Washing
Technical Illustrator

Advertising Information
Steve Bossert, K2GOG
Business Services
860-594-0203 – Direct
800-243-7768 – ARRL
860-594-4285 – Fax

Circulation Department
Cathy Stepina
QEX Circulation

Offices
225 Main St., Newington, CT 06111-1400 USA
Telephone: 860-594-0200
Email: **qex@arrl.org**

Subscription rate for 6 print issues:
In the US: $29

US by First Class Mail: $40

International and Canada by Airmail: $35

ARRL members receive the digital edition of *QEX* as a member benefit.

In order to ensure prompt delivery, we ask that you periodically check the address information on your mailing label. If you find any inaccuracies, please contact the Circulation Department immediately. Thank you for your assistance.

November/December 2025

About the Cover

Hajime Nakajima, JR1OAO, developed an innovative tuning design for his magnetic loop antenna that offers full HF coverage, 100 W capability, and flexible loop configurations in antenna restricted environments in "Desktop MLA."

In This Issue:

Index of Advertisers

The American Radio Relay League

The American Radio Relay League, Inc., is a noncommercial association of radio amateurs, organized for the promotion of interest in Amateur Radio communication and experimentation, for the establishment of networks to provide communications in the event of disasters or other emergencies, for the advancement of the radio art and of the public welfare, for the representation of the radio amateur in legislative matters, and for the maintenance of fraternalism and a high standard of conduct.

ARRL is an incorporated association without capital stock chartered under the laws of the state of Connecticut, and is an exempt organization under Section 501(c)(3) of the Internal Revenue Code of 1986. Its affairs are governed by a Board of Directors, whose voting members are elected every three years by the general membership. The officers are elected or appointed by the Directors. The League is noncommercial, and no one who could gain financially from the shaping of its affairs is eligible for membership on its Board.

"Of, by, and for the radio amateur," ARRL numbers within its ranks the vast majority of active amateurs in the nation and has a proud history of achievement as the standard-bearer in amateur affairs.

A *bona fide* interest in Amateur Radio is the only essential qualification of membership; an Amateur Radio license is not a prerequisite, although full voting membership is granted only to licensed amateurs in the US.

Membership inquiries and general correspondence should be addressed to the administrative headquarters:

ARRL
225 Main St.
Newington, CT 06111 USA
Telephone: 860-594-0200
FAX: 860-594-0259 (24-hour direct line)

Officers

President: Rick Roderick, K5UR
P.O. Box 1463, Little Rock, AR 72203

The purpose of *QEX* is to:

1) provide a medium for the exchange of ideas and information among Amateur Radio experimenters,

2) document advanced technical work in the Amateur Radio field, and

3) support efforts to advance the state of the Amateur Radio art.

All correspondence concerning *QEX* should be addressed to the American Radio Relay League, 225 Main St., Newington, CT 06111 USA. Envelopes containing manuscripts and letters for publication in *QEX* should be marked Editor, *QEX*.

Both theoretical and practical technical articles are welcomed. Manuscripts should be submitted in word-processor format, if possible. We can redraw any figures as long as their content is clear. Photos should be glossy, color or black-and-white prints of at least the size they are to appear in *QEX* or high-resolution digital images (300 dots per inch or higher at the printed size). Further information for authors can be found on the Web at **www.arrl.org/qex** or by e-mail to **qex@arrl.org**.

Any opinions expressed in *QEX* are those of the authors, not necessarily those of the Editor or the League. While we strive to ensure all material is technically correct, authors are expected to defend their own assertions. Products mentioned are included for your information only; no endorsement is implied. Readers are cautioned to verify the availability of products before sending money to vendors.

Ron Diehl, NQ8W

Perspectives

The breadth and depth of communication science and technology in amateur radio could not be better illustrated than in this issue of *QEX*. Each contribution reflects a distinct aspect of our craft: reinforcing our grasp of fundamentals, applying ingenuity to practical challenges, and exploring innovative technologies that promise to change the way we operate.

We return to one of the cornerstones of electronics. Inductance remains vital in everything from filters and baluns to transformers and resonant circuits, yet it is often not as well understood as resistance or capacitance. A clear treatment of its principles and applications helps experimenters design with confidence and connect theory to practice.

Another feature highlights the enduring value of logarithmic methods. Once embodied in mechanical slide rules and later in handheld calculators, these mathematical tools continue to shape circuit implementations today. Tracing their evolution reminds us that much of modern engineering rests firmly on foundations laid decades ago, and that the clever insights of earlier generations still influence our workbench.

Innovation also appears in the antenna realm, where amateurs often confront severe space and location restrictions. One author shows how a compact loop design can deliver surprising performance from a desktop environment. This type of creative engineering shows that physical limitations need not prevent world-class operating, and that effective solutions are often within reach of any determined experimenter.

Finally, we look ahead to the fast-growing impact of artificial intelligence. Neural networks, once confined to research laboratories, are now practical tools for recognizing and classifying the multitude of signals that fill the shortwave spectrum. By adapting these techniques to amateur applications, we gain powerful new ways to monitor, analyze, and better understand the radio environment.

From fundamental physics to emerging machine intelligence, from historical methods to clever solutions for everyday constraints, this issue underscores the remarkable diversity of amateur experimentation. Whether your focus lies in careful measurement, creative design, or forward-looking technologies, you'll find ideas here to challenge and inspire your own work.

Writing for *QEX*

QEX is a forum for the free exchange of ideas among communications experimenters. *QEX* is published bimonthly.

Please send full-length *QEX* manuscripts, or share a Technical Note of several hundred words in length plus a figure or two, to **qex@arrl.org**. We pay $50 per published page for full articles and *QEX* Technical Notes. Get more information and an Author Guide at **www.arrl.org/qex-author-guide**. If you prefer postal mail, send a business-size self-addressed, stamped (US postage) envelope to: *QEX* Author Guide, c/o Margie Bourgoin, ARRL, 225 Main St., Newington, CT 06111.

Tak Asami, W6SI (article), and Hajime Nakajima, JR1OAO (antenna design)
desktopmla@w6si.com

Desktop MLA

This compact desktop magnetic loop antenna offers full HF coverage, 100 W capability, and flexible loop configurations, bringing real performance to even the most antenna-restricted environment. The design received an Honorable Mention in the 2024 *QST* Antenna Design Competition. See recent issues of *QST* for other competition honorees.

Introduction

From my earliest days of amateur radio activities, erecting HF antennas has always been a problem. Today, despite owning my own house, the situation is not much better with heavy antenna restrictions.

Trying to build an antenna that is useful and versatile has been a lifelong project for me. The entry presented here is a small loop antenna with flexible configurations that covers all HF bands, yet it can sit on a small tabletop (see **Figure 1**) Despite its appearance, this is not a toy, but a practical all-band antenna with great utility and performance.

Figure 1 – Desktop MLA setup in the back yard of W6SI.

This antenna was developed by Mr. Hajime Nakajima (JR1OAO), and a group of technical hams based in Yokohama, Japan **[1]**. This collaboration has existed since 2016.

The antenna consists of a base unit in a plastic casing, and a 1 m diameter loop antenna element, which consists of LMR-400 coax cable supported by a PVC mast. The loop element is exchangeable with different size loop diameters to target different bands and efficiency. Notable features include:

- supports multiple configurations to cover the 80-to-10-meter ham bands
- supports up to 100-watt transmission power
- enables reliable and stable operations even from the most antenna restricted environment
- the compact base unit is ultimately portable
- built-in matching system supports remote manual control as well as automated tuning

Small loop antennas, a.k.a. magnetic loop antennas, are nothing new. The need for relatively large capacitors with high voltage tolerance made them difficult to build. They are often limited to low power levels of 5 to 10 watts and considered not practical for their low radiation efficiency and narrow usable SWR bandwidth.

Desktop MLA has addressed most of these issues. Several people reported good operating experience using it. Other than the custom-made variable capacitor, it does not use any difficult-to obtain parts or esoteric construction techniques that discourage anyone from building one. I have built several units that are in use proving how easily they are produced, easy to use, and good performers.

The Build and Variable Configurations

Overview

The set of capacitors, the small DC motors, and position sensing potentiometers are housed in a plastic casing of

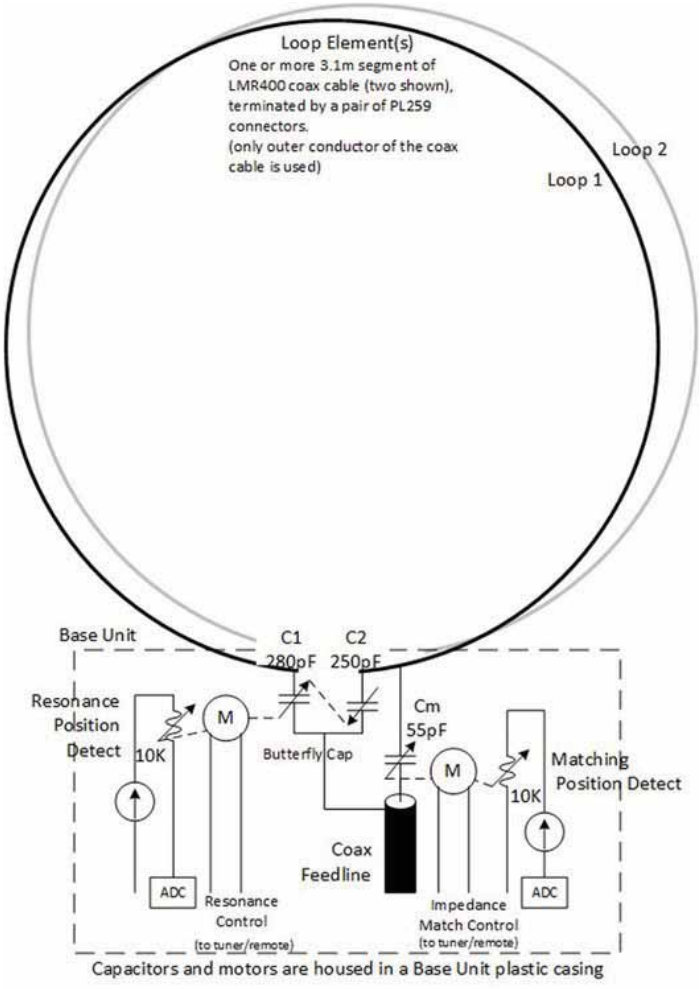

Figure 2 – Simplified schematics of Desktop MLA.

22 × 22 × 11 cm. This is the base unit. Attached on the top is the coaxial cable loop element. It is supported by a 26 mm PVC pipe a little over 1 m tall (depending on the size of the elements used) (see **Figure 2**).

Loop Configurations

The loop elements are readily changed to meet operational requirements. **Figure 3** shows two 1 m diameter coax loops in parallel, attached to the base unit. This is a popular configuration that matches the 20 m to 15 m bands. It is known that parallel elements can enhance radiation efficiency compared to a single loop.

Figures 4 and **5** show various loop element configurations to cover different bands. One of the reasons this configuration cannot reach higher bands (12 m, 10 m and beyond), is the minimum capacitance for the tuning capacitor is too large. To go to the higher bands (12 m, 10 m bands and beyond), shorter loop elements must be used. A 70 cm diameter loop can be used for up to the 10 m band. **Figure 6** is a 30 cm diameter loop setup for the 6 m band.

Configuration change does not require any tools. The feed point is readily reachable at the tabletop, or tripod (**Figures 7** and **8**). Because the loop antenna is in vertical orientation (with respect to ground), it is ground independent and does

Figure 3 –Two loops, 1 m diameter configuration of Desktop MLA.

not require height to radiate effectively. This is a distinguishing feature of this type of antenna.

The loop element uses only the outside conductor of the cable. The center conductor is not connected. I used LMR400 cable because of its thick solid inner conductor keeps the loop shape, is self-supportive, and does not require horizontal support at the middle. When two or more elements are used in parallel, the distance between the elements is optimal if kept between 50 mm and 80 mm. Closer or further tends to affect the radiation efficiency negatively. Cable management and top support makes use of 3D-printed custom brackets (**Figure 9**). For two loop elements, six cable spacers and top support is needed.

The Base Unit

The base unit (**Figure 10**) houses the tuning element for the system. The matching technique used is referred to as "c-coupled." It is derived from the original Patterson match. Notice it does not use a small coupling loop typical of MLA implementation. C-coupled match allows heavy components like the tuning capacitor to be concentrated at the bottom. This avoids making the loop antenna top heavy, enabling a unit so compact it can be placed on a tabletop without support. C1 and C2 are wired in series to resonate the loop to the transmission frequency. Parallel combination of C2 and Cm is used to match the feedline impedance (50Ω) to the radiation impedance of the loop (~0.1 Ω). The capacitor is unique in the sense that three capacitors are integrated into a single component. It has two axes of rotation, for C1/C2 and Cm, to perform resonance and impedance match, independently.

One of the important points to note is that the outer conductor of the feedline coax is not the neutral point. This could cause some common mode current on the feedline to affect matching

Figure 4 – Configuration for two parallel single loops for 20 m to 15 m bands.

Figure 5 – Configuration for one series two-turn loop for 40 m and 30 m bands.

and radiation. It is strongly recommended to insert a good common mode filter on the feedline cable.

During transmission, very high RF voltage (~4 KV) develops and large RF current flows through the loop element, therefore it is not feasible to perform tuning manually, for RF safety's sake. The unit is equipped with a pair of small DC motors (**Figures 11,12**) to tune the capacitors remotely. A remote control with batteries and switch box is easy to build and operate. The motor mechanism also has a slider potentiometer synchronized with the rotation, so the capacitor position can be sensed by measuring the resistance. It is to be used with an auto tuner.

Motorized Section Details

Because of the high-Q nature of the antenna, the usable bandwidth at a given point is very narrow. The slightest change in transmission frequency calls for re-tuning. It is also subject to temperature/humidity change even without frequency shift. While this is not a big problem for digital mode where you tend to stay in a narrow frequency range, more agile modes such as SSB, CW and RTTY can benefit from automated tuning.

Figure 6 – Two loop, 30 cm diameter configuration for 6 m band.

Working with another colleague **[2]**, we built an automatic tuner named DPAT. This is a sophisticated system that continuously monitors the RF voltage and current through the coax during transmission, to keep adjusting the match. But that is a different subject and will not be discussed here in detail. If the reader is curious, a brief introduction of this tuner is available at **QEXfiles.** The point is, the unit has a motorized mechanism to support such automated tuning. Without the auto tuner, the same mechanism can use an AA-battery powered switch to facilitate manual tuning. By applying 3 VDC to two motors in

Table 1 – Bottom Unit Parts List

Component	Material	Specifications			Quantity
Attachment "L"	Aluminum	100 mm x 30 mm		t = 1 mm	2
SO-239 receptacle		Bulk head			4
Butterfly Capacitor	Aluminum	As specified below			
Mast Support	PVC	26 mm id, 45 mm h			
Screws	Aluminum	M5	For "L" and capacitor attachment		4
		M4	For Mast Support attachment		4
Nuts	Aluminum	M5	For "L" and capacitor attachment		4
		M4	For Mast Support attachment		4

Figure 7 – Single three-turn loop configuration for 80 m band.

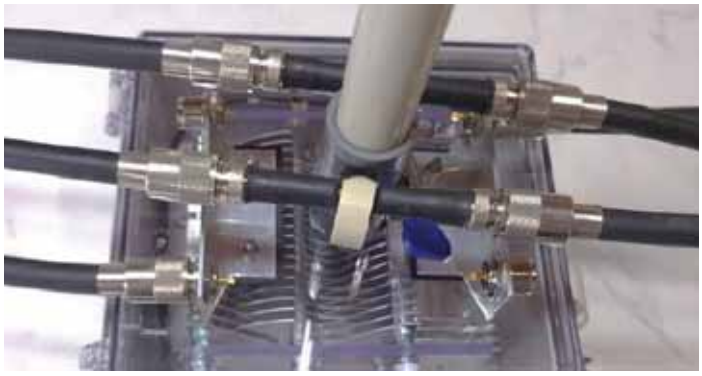

Figure 8 – Three coax loops are connected in series.

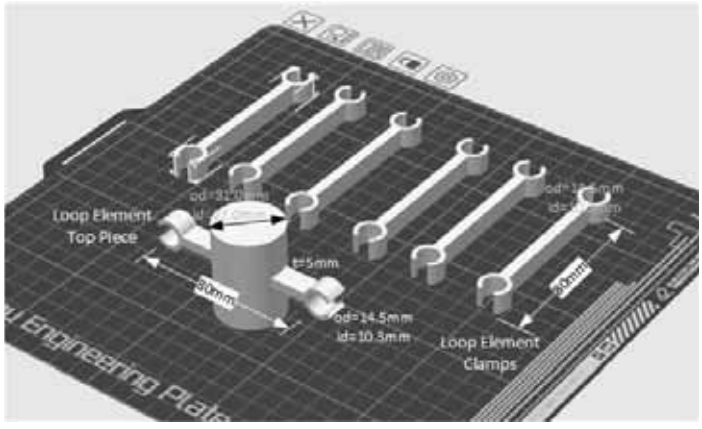

Figure 9 – 3D-printed element clamp parts.

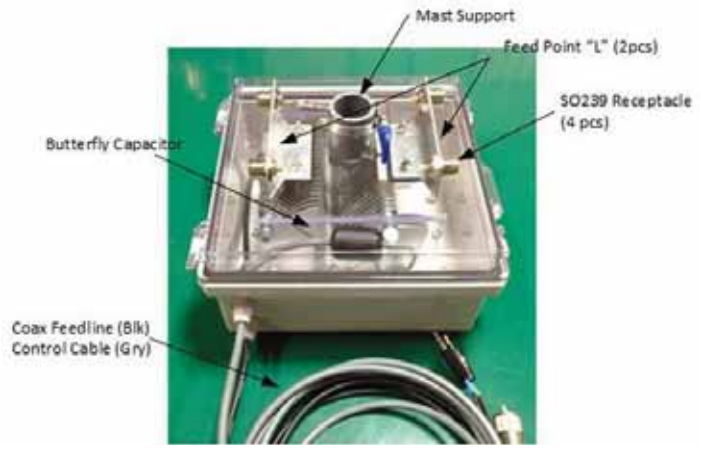

Figure 10 – Base Unit.

the base unit, you can turn the variable capacitor to the desired frequency and impedance to match (**Figure 13**).

Construction

Base Unit

As stated earlier, the base unit contains resonance and matching capacitors, motor mechanisms, the element attachment brackets, and the mast support at the top (**Figure 14**, **Table 1**).

Butterfly Capacitor

One of the key components of the matching system is the butterfly capacitor with the third small capacitor integrated. As the schematic diagram (Figure 2) shows, the C-match system consists of three capacitors, two of the series connected capacitors C1 and C2, serve as tuning elements. The third, Cm, is the impedance matching capacitor. It has dual axis tuning where antenna resonance and impedance matching are done separately to achieve the highest level of match, near SWR=1.0 in most cases.

The capacitor is custom built by the MLA48 Project group members. Though special skills and tooling are necessary to build those capacitor blades, a similar Butterfly Capacitor kit (less the third capacitor) can be found in the open market **[3]** if one would like to build one himself. (Note: **Figure 15** is similar to open market butterfly capacitor that does not have the third capacitor. The inventor does not have a concise drawing for the integrated unit. He built it on the fly.)

The construction details of the capacitor are shown in **Figure 16, Table 2.** This is the special version created by Mr. Nakajima that integrates the tuning (C1 & C2) and the matching (Cm) capacitors into a single unit. C1 and C2 share the single axis of rotation that is turned by a DC geared motor, while Cm (consists of 3 rotator blades that are half size of butterfly blades) is turned by another motor in the similar mechanism, as shown in Figure 13.

One of the reasons most MLA antennas come with low power limitation is the high voltage tolerance required of the tuning capacitor. This Butterfly capacitor has 1.5 mm clearance

between stator and rotator blades. The breakdown voltage of air is 3.0 kV/mm. Hence, the estimated DC tolerance of C1 and C2 with 1.5mm clearance is 4.5 kV.

During 100-watt transmission, the gap voltage across the loop element can exceed 4 kV. But because C1 and C2 are connected series, only half of that voltage shows up at the capacitor blades, or 2 kV. With more than 100% margin to cover for RF arcing, it is, by design, 100 watt tolerant.

Simulations and Testing

Simulations

The usual model or mini-nec models are not given. All simulations on this antenna were performed using a professional EM field simulator S-NAP Wireless Suite(R) provided by MFJ Inc. **[4]** to closely analyze interactions in near-field, necessary to ascertain behaviors of this type of antenna. A more detailed simulation result for the antenna is provided in a separate file, (DesktopMLASims.pdf) available at **QEXfiles**.

Summary of the simulations (configurations, radiation efficiency, actual implementations):

- 7 MHz, Single Two-turn loop, 1 m diameter loop
  Efficiency = 13.9% (Figure 5)
- 7 MHz, Single Two-turn loop, 1.3 m diameter loop
  Efficiency = 23.2% (Figure 5)
- 14 MHz, Two Parallel Single-turn loop, 1 m diameter
  Efficiency = 54.1% (Figure 4)
- 21 MHz, Two Parallel Single-turn loop, 1 m diameter
  Efficiency = 83.65% (Figure 4)
- 28 MHz, Single Two-turn loop, 70 cm diameter
  Efficiency = 76.5% (Figure 4)
- 3.5 MHz, Single Three-turn loop, 1 m diameter
  Efficiency = 2.45% (Figure 7)

Each configuration is adjusted to match SWR < 1.1 both in simulation and actual implementation.

The report covers S11 (equivalent of SWR) for impedance match and radiation efficiency for a given set of configurations. The effective SWR bandwidth is very narrow, but it is not considered a problem since the antenna is easily tunable. S11 of -30 dB is equal to a VSWR of 1.05. Anything beyond that can be considered a "perfect match". S11 of -9.5 dB is a VSWR of 2.0. That defines the usable bandwidth of the tune.

The simulations show the antenna is truly omni-directional, except for void at the top for lower bands. It means the vertically oriented loop is suitable for local as well as DX communications.

The simulations are performed for free space, but due to its relatively ground independent nature, the directionality characteristic does not change much for ground simulations.

The computed radiation efficiency for two 1 m diameter loops varies from 14% for 7 MHz (single two-turn loop) to 76.5% for 28 MHz (two parallel loops). Longer loops give better efficiency. That means for the same antenna, the behavior changes from mostly magnetic to magnetic–electric hybrid.

Testing

A separate report on initial tuning results, InitialTuningTestOnDesktopMLA.pdf, is available at **QEXfiles.**

To summarize, two parallel, single turn loops of 1 meter diameter was tuned from 8.9 MHz to 24.2 MHz It is confirmed that it is tunable on 30 m, 20 m, 15 m bands. I did not try 12 m and 10 m bands, as a shorter 70 cm loop element was not prepared. A single two-turn loop of 1 meter diameter was tuned from 4.75 MHz to 9.5 MHz It is confirmed that it is tunable on the 40 m band. Each ham band on the tuning range was shown to match

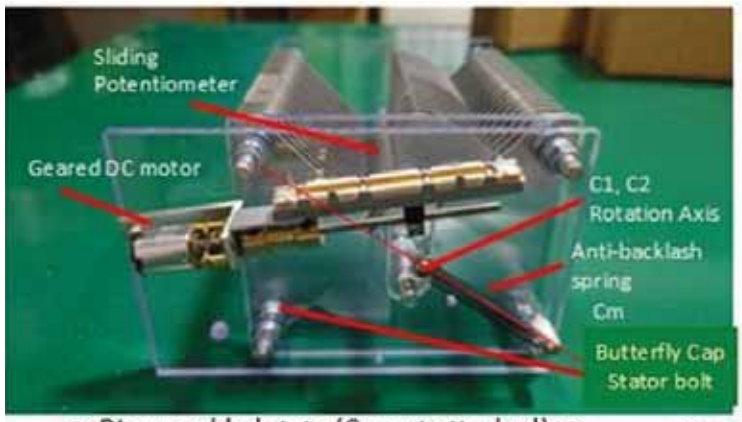

Figure 11

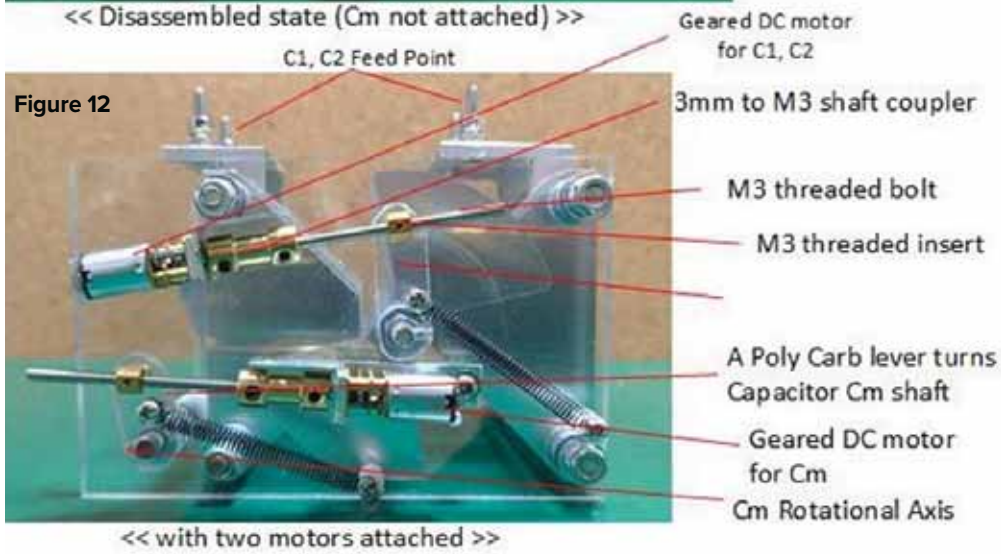

Figure 12

Figure 11 – Disassembled state (Cm not attached).
Figure 12 – With two motors attached.

Table 2 – Butterfly capacitor parts list					
Component	**Material**	**Specification**			**Quantity**
Rotor Blades	Aluminum			t = 1 mm	20
Stator Blades	Aluminum			t = 1 mm	40
Spacers	Aluminum	M5	d = 10 mm	t = 4.0 mm	100
				t = 2.5 mm	1
				t = 1.5 mm	1
Threaded bolts	Unichrome	M5		l = 150 mm	4
				l = 170 mm	1
Nuts		M5	d = 10 mm	t = 4 mm	24
Washer		M5	d = 12 mm	t = 0.8 mm	36
Spring Washer		M5	d = 9.2 mm	t = 1.3 mm	24
Frames	Polycarbonate	h = 88 mm	84 mm x 100 mm	t = 5 mm	2
Geared DC motor		3 V, 30 rpm			2
Threaded bolts		M4		l = 895 mm	2
Shaft Joint		3 mm to M4			2
Slider potentiometer		Bourns PTA6043-2010DPB203 10K			2
Threaded Insert		Various vendors, M4 threaded insert			2
Rotation Lever	Polycarbonate	Custom			2

with a low SWR. With these two configurations, this antenna covers 40 m to 15 m bands consecutively.

Though not tried, it should tune to the 60 m band, and with a shortened 70 cm diameter, it should tune to 10 m and perhaps to 6 m as well. 80 m using a three-turn loop was not tried to date, mainly due to lack of cable inventory. All measurements were performed using a nanoVNA.

Actual Usage

This section shows various setups used on this antenna for multiple purposes. For portable setups, since it disassembles easily between the base unit and the loop elements, it is easy to carry and deploy quickly. If there is a picnic table near the operation site, base supports like tripods are not necessarily needed (**Figure 17**).

Permanent or semi-permanent deployment is easily accomplished. I have included images of working installations from actual users. The pictures and names are used with permission from individuals.

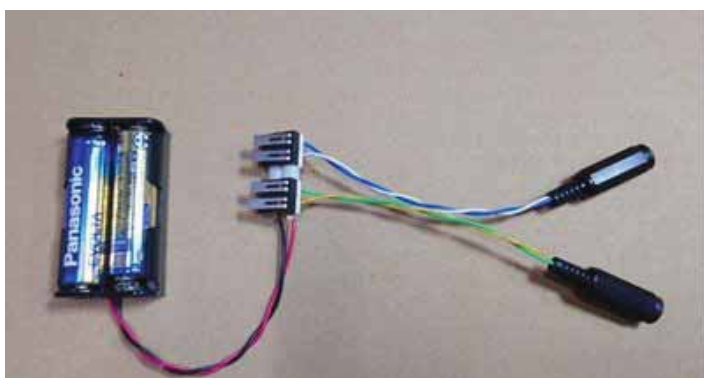

Figure 13 – A battery-based manual remote tuning controller.

Figure 18 shows Mr. Yonosuke Harada's DXCC achieving MLA setting. Being one of the most active MLA users, he has arrays of different small loop antennas deployed at home. The desktop MLA is placed at the front (left most, behind a square loop). He is one of the practitioners of MCB (MLA-Coupled Beam) antenna. He couples two or more small loop antennas to form strong directional pattern and gain. This is a separate subject worthy of discussion. He has been using small loop antennas since 2016 to challenge DXCC. He operates a 100-watt station using these small antennas. As of May 2022, he has made 10,500 contacts, mostly using digital and CW all on his array of small loops.

Figure 19 shows a Desktop MLA on top of minivan. Placed vertically on the top of the roof, it provides good portable operation experience without the hassle of setting up an antenna with good height. It works well but it is for stationary operation; it is hazardous to drive with the loop erected vertically, and a horizontally mounted antenna does not work well.

On the Air

It is often said that small loops are not practical for DX due to low radiation efficiency. Narrow bandwidth makes it hard to use on frequency agile modes like SSB, CW and RTTY. Difficulty supporting high power transmission also limits DX opportunity.

Desktop MLA is developed to overcome these shortcomings to ease the use of this remarkable antenna. Actual user comments include, the antenna "hears" very well, and the low radiation efficiency is not much worse than many of the short-

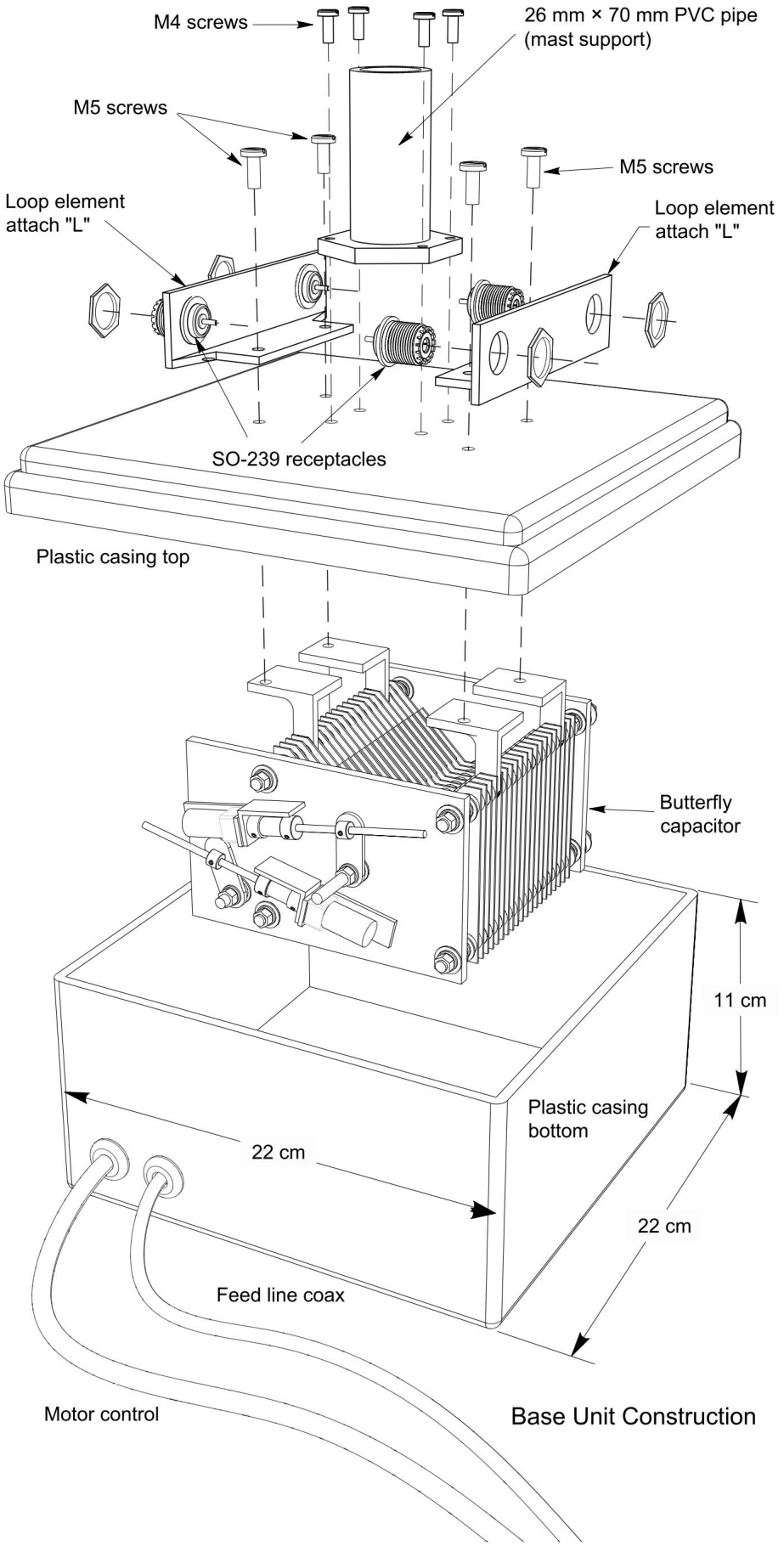

Figure 14 –Illustration of Desktop MLA base unit construction.

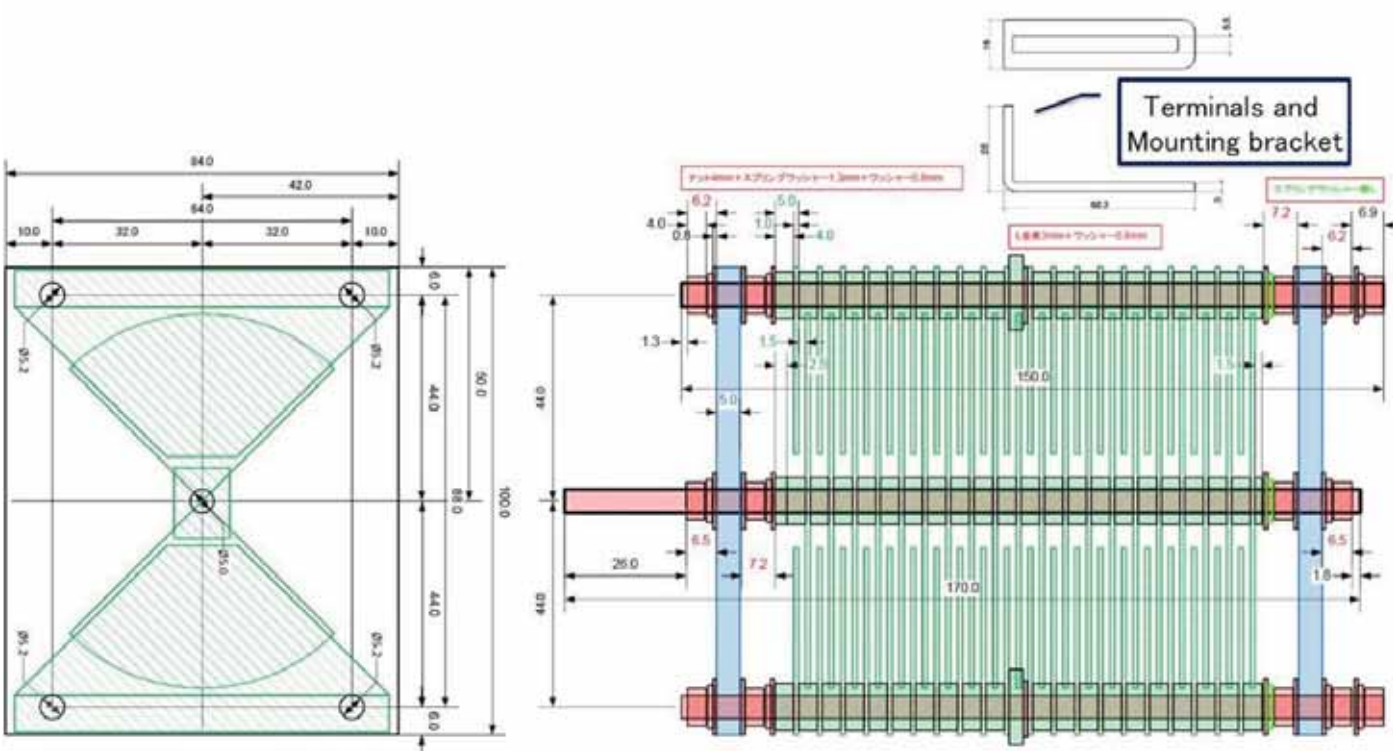

Figure 15 – Butterfly capacitor drawings. [courtesy Mr. Hiroyuki Uchida / JG1CCL]

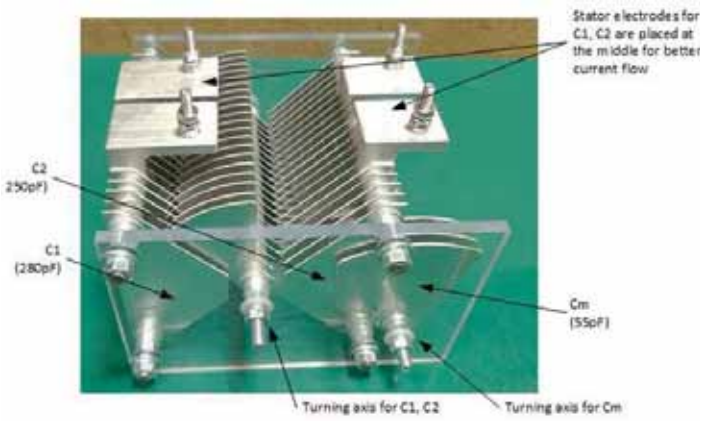

Figure 16 – Construction details of butterfly capacitor.

ened antennas with insufficient height (many of us just don't know that fact).

It certainly is not a miracle antenna beating out big beam kilowatt stations. But like any other antennas, operation skills count. In general, if I can hear him, there is a good chance I can work him. Given good propagation, just a few watts can reach almost everywhere on Earth.

Conclusion

This remarkable antenna is easy to deploy, easy to work with, and performs well in very restrictive environments. Please note this is not a one-off experiment. It is a very reproducible design, and JR1OAO encourages anyone who can build this to try and keep improving it. Through this discussion, I hope to

Figure 17 – Desktop MLA deployment at JS1EYR (Mr. Katsuyoshi Akazawa).

Figure 18 – Mr. Yonosuke Harada's, JA3UOQ, DXCC-achieving MLA setting.

have impressed upon the reader, the usefulness and craftsmanship of this design.

Acknowledgement

The creator of the project wants to thank Tak Asami, W6SI, for his efforts in documenting his work on Desktop MLA development. He also would like to thank members of the MLA-48 group for their contributions on building, simulation support, and conducting on-air tests for the project, which is still ongoing.

Additional reports mentioned in this article are available at **www.arrl.org/QEXfiles**.

Editor's Note: As highlighted in this article, the antenna operates at high voltages that can be easily accessed during operation. It is imperative to exercise extreme caution and avoid any contact with antenna components while transmitting. Additionally, please adhere to the FCC regulations regarding Maximum Permissible Exposure (MPE). According to CFR 97.13(c), we are required to limit RF exposure in accessible areas.

Hajime Nakajima, JR1OAO, is a graduate of Yokohama National University, School of Engineering, Electrical Engineering. In college days, aside from engineering study, he was active in a male chorus group and built his own audio tape recorder to record their singing. This led him to get a position at SONY. He worked for SONY Corporation (1978~2012), developing aviation radar systems, high resolution CTV, and PC displays. Now retired, he is an active developer and researcher for the MLA-48 group. Originally licensed in 1970 as JR1OAO, he currently holds a Japanese 1st Class Amateur Radio Operator license. He is a winner of six JARL Ham Fair DIY contest awards.

Figure 19 – JR1OAO's own desktop MLA mobile operation.

Notes

[1] MLA48 Project, led by JG1UNE Dr. Hiroaki Kogure is "the group of people who love MLAs," Access their website at http://home.j00.itscom.net/kce/J/MLA48.html.

[2] JA9BQE Mr. Shuichi Hashiba developed original idea and several members of MLA48 Project contributed.

[3] TA1LSX / TA2WK Butterfly capacitor kit (aluminum plate) can be found on eBay and Etsy.

[4] License provided and supported by Dr. Takahiro Ogawa (JA5KVK).

Note the material size, especially the thickness, is important to ensure solid, stable build of the capacitor. Using incorrect thickness parts can result in shorting blades.

José Luis Giordano, CE4TW
Hist. René León E. 300, DP201, Curicó, 3341718, Chile | **JLGiordano@hotmail.com**

About Inductance: What Every Amateur Should Know

Inductance is a fundamental property in transformers, baluns, chokes, and filters, although its function is often misunderstood. This article explains its origin, properties, and applications, and also summarizes the theoretical and practical formulas for designing and calculating solenoids and toroids, or for using online calculators with confidence.

Introduction

In repair, design, and assembly work carried out in the amateur radio workshop, it is common to deal with devices and circuits that have inductive elements, such as voltage boosters, transformers, impedance adapters, baluns, chokes, traps, and loading coils. A fundamental part in these examples is the coil whose design focuses on the calculation of *inductance*, a physical quantity not as well understood as resistance or capacitance. Furthermore, in almost all cases, even in the simplest solenoid, the calculation of inductance is usually very complicated. For this reason, many radio amateurs use calculators implemented on internet pages without having a reference to know if this tool would give them correct values in other situations.

The aim of this work is to use simple but rigorous language to give greater knowledge to the radio amateur who wants to experiment, so that he can design and assemble inductors with confidence in the tools used.

Part I – PROPERTIES AND APPLICATIONS OF INDUCTANCE

In this first part, the origin, properties, and effects of inductance are explained, introducing the definitions, units, and main concepts required by the applications.

Electric current effects

The passage of electric current through a conductive wire has thermal and magnetic effects and if the current is variable, electromagnetic effects. Due to the resistivity of the material there is an irreversible loss of energy in the form of heat (according to *Joule's Law*). This heat increases the temperature of the wire material resulting in dissipation to the outside. On the other hand, electric current is surrounded by (closed) magnetic field lines (quantitatively related according to *Ampère's Circuital Law*). Therefore, some of the electrical energy delivered to the conductor is lost as heat and another part is stored in the magnetic field. In addition to these two effects, which are always present, the wire has a reactive behavior to the variation of current caused by electromagnetic induction (*Faraday's Law of Induction and Lenz's Law*). The intensity of this reaction depends on a parameter called self-inductance, or inductance.

It should be noted that electromagnetic induction is one of the most beautiful and important phenomena in nature. It is the foundation of the electrical generator with which wind, hydraulic, thermal, , and nuclear energy are converted into electricity. It was discovered by the autodidact English scientist Michael Faraday (1791–1867) in 1831, and its understanding was completed three years later by the Russian physicist Emil Lenz (1804–1865), by whom in the formulas, inductance is symbolized by L.

What inductance is and how it works

Within a circuit, the inductance of a coil is a parameter that represents its **tendency to oppose the change in the current** circulating in it. Let's consider the simplest coil: a **thin solenoid**. This coil is cylindrical, formed by a single layer of N identical circular turns and a surface A, with thin wire compactly wound, surrounded and filled with a homogeneous non-conductive material with magnetic permeability μ (In this analysis we will not consider the electrical resistance of the coil wire). An electric current I, flowing through the wire produces a magnetic field $B(I)$ inside the solenoid (Here

we write $B(I)$ to emphasize that the value of B depends on the value of I). The field generated by the current crosses the surface of each turn, producing a magnetic flux $AB(I)$ through each one, and a total flux $\phi(I) = NAB(I)$ in the coil. If in an infinitely small period Δt the current intensity I changes by an amount ΔI, the field changes by an amount ΔB. Consequently, there is a $\Delta\phi = NA\Delta B$ change in the flow. Due to electromagnetic induction, the rate of change of the flux $\Delta\phi/\Delta t$ determines the voltage induced at the coil terminals, which can be broken down into two factors:

$$V_L = \frac{\Delta\Phi}{\Delta t} = \left(\frac{\Delta\Phi}{\Delta I}\right)\left(\frac{\Delta I}{\Delta t}\right)$$

The first factor is the inductance L of the coil:

$$L = \frac{\Delta\Phi}{\Delta I} \qquad \textbf{Equation 1}$$

which represents how the magnetic flux $\phi(I)$ changes when the intensity I of the current changes. Inductance does not depend on I. It only depends on the magnetic material and the geometry of the coil. Furthermore, from the above, it is seen that inductance is the constant of proportionality between the voltage and the rate of change in current:

$$V_L = L\frac{\Delta I}{\Delta t} \qquad \textbf{Equation 2}$$

Therefore, if $\Delta I/\Delta t$ is very large, the voltage V_L will also be large. This is the basis for the operation of many ignition devices that generate high voltage with short pulses of current. Two familiar examples are the electric arc in fluorescent tubes (where the plasma is achieved by the high voltage produced by the inductance of the *ballast*), and the spark from the spark plugs in automobile combustion engines (due to the high voltage generated with *ignition coil*).

The coils can store magnetic energy, which corresponds to the magnetic field associated with the current. Calculating the energy from the field would be quite difficult because the field changes at every point in space, but it can be calculated from the current. In fact, by analyzing the circuit, it can be shown that if the current has an intensity I, the associated magnetic energy E_{mag} is given by:

$$E_{mag} = \frac{1}{2}LI^2 \qquad \textbf{Equation 3}$$

An important application is found in circuits called "Boost Voltage Converter" or "DC-to-DC Voltage Boost", where the energy stored in the inductance allows the continuous voltage to be raised by a few volts (without using a heavy transformer which also would require alternating current). For example, some radio amateurs use a boost converter to feed 13.8 V to a transmitter using a 12 V car battery.

On the other hand, in the case of alternating current of frequency f, the opposition of the inductance to the change in current in the circuit is manifested with an inductive reactance given by:

$$X_L = \omega L \qquad \textbf{Equation 4}$$

where $\omega = 2\pi f$ is called **angular frequency**. This makes the existence of the coil favorable for low frequencies (fewer ohms of reactance), and unfavorable for high frequencies (higher X_L). Based on this property, inductances are used in a wide variety of chokes, and high-pass, low-pass, band-pass, and notch filters. Another example is antenna tuners where **Equation 4** shows that to achieve a similar inductive reactance (associated with the impedance range that the tuner can adapt), in the low bands (lower frequencies) a greater inductance is necessary. Therefore, the largest inductance with which a tuner is designed is determined by the lowest operating frequency (in addition to the power and adaptation range).

Summing up, it can be said that the main properties of inductance for use in amateur radio are described with the latest expressions: **Equation 1** shows what it is and what it depends on, and **Equations 2**, **3**, and **4** respectively indicate that the voltage, magnetic energy and inductive reactance are proportional to L. Furthermore, Equations 4 and 2 show that if there is no change in current, there is no reactance or voltage across L.

There are other important applications of inductance such as those that use their ability to *delay* current with respect to voltage (unlike capacitors) and have resonance with capacitances. These two properties are based on the fact that the inductive reactance given in Equation 4, is a *positive* number *directly* proportional to the frequency f, while the reactance $X_c = -1/(\omega C)$ of a capacitor is the opposite, that is, it is *inversely* proportional to f and is also a *negative* number. (although many authors *incorrectly* call capacitive reactance, $1/(\omega C)$, without the sign).

Units and general expression of inductance

In the International System of Units (S.I.), the magnitude B of the magnetic field and the magnetic flux ϕ are measured, respectively, in *tesla* (T) and in weber (Wb). Therefore, there is the following equivalence between units: $Wb = m^2T$. On the other hand, time, voltage and intensity of electric current are measured respectively in second (s), volt (V) and ampere (A). Then, since inductance is measured in henry (H), it turns out that $H = Wb/A$. The name of this unit honors the American scientist Joseph Henry (1797–1878) who discovered self-induction and mutual induction independently of Faraday, although without publishing it beforehand. On the other hand, since the reactances X_L and X_C are measured in ohm (Ω), the capacitance in farad (F) and the angular frequency ω in $1/s$, then $\Omega = H/s$ and also $\Omega = s/F$.

Equation 1 allows deducing the dependence of L on N and μ for most cases. The intensity B of the magnetic field is proportional to the number of turns, $B \propto N$, and then, since $\phi = NBA$, it turns out that $\phi \propto N^2$, that is, the inductance is always propor-

tional to N^2. On the other hand, if the magnetic permeability μ increases, the concentration of field lines also increases and in the same proportion. Therefore, the field intensity B and the flux ϕ are proportional to μ and then the inductance as well. In this way we see that for simple coils, we can always express their inductance in the form:

$$L = \mu G N^2$$

where G is a geometric factor. In the S.I., the permeability μ is measured in henry/meter (H/m) and then the geometric factor G is measured in meter. In applications it is preferred to use the *relative* permeability defined by:

$$\mu_{rel} \equiv \frac{\mu}{\mu_0}$$

where $\mu_0 = 4\pi \times 10^{-7}$ H/m is the magnetic permeability in a vacuum (a universal physical constant). For example, the initial permeability of Ferrite Mix 43 is $\mu \approx 0.001$H/m, but it is preferred to use $\mu_{rel} \approx 800$. If there is no magnetic material in the coil, $\mu = \mu_0$ and then $\mu_{rel} = 1$.

It is common in amateur radio for inductance to be expressed in microhenry (μH). Therefore, in this work, when expressing L in μH, "$L(\mu\text{H})$" will be indicated. For this, the vacuum permeability is expressed as:

$$\mu_0 = \frac{2\pi}{5}\frac{\mu\text{H}}{\text{m}} \qquad \textbf{Equation 5}$$

and then $\mu = \mu_{rel}(2\pi/5)$ μH/m, so:

$$L(\mu H) = \frac{2\pi}{5}\mu_{rel} G N^2 \frac{\mu\text{H}}{\text{m}}$$

where length can be expressed in millimeter, centimeter, inch, etc. changing G/m for the corresponding equivalence:

$$\frac{G}{\text{m}} \equiv \frac{G(\text{mm})}{10^3\,\text{mm}} \equiv \frac{G(\text{cm})}{10^2\,\text{cm}} \equiv \frac{G(\text{in})}{39.37\,\text{in}} \equiv \ldots$$

Inductance factor

With good approximation, the G factor can be easily calculated in an infinitely long cylindrical coil and in a toroidal coil of very small section. However, in almost all other cases, the calculation of G (and L) is very complicated because the magnetic field lines are always closed. These lines go around coming out of the north magnetic pole at one end, opening up and converging again to enter through the south pole at the other end. This means that the magnetic field inside a solenoid is not uniform (and therefore the flux expression ϕ=NAB is only approximate). The non-uniformity of the field is more pronounced when the solenoid is too short, or the winding is close to one of the two ends of the core, or when the wires are very thick in relation to the radius of the solenoid, or the material of the core has lower permeability.

Additionally, in radio frequency (RF) applications, there are other effects that further complicate the calculation of L. A direct current (DC) flowing in a wire is distributed uniformly throughout the cross section of the conductive material, penetrating to the center. However, at high frequencies the current attenuates as it penetrates into the conductor, so the current flows only in a very thin surface layer. This electromagnetic phenomenon is known as the *skin effect*, and it is the main phenomenon responsible for the increase in losses in transmission lines with increasing frequency. Additionally, for very high frequencies, the skin effect is modified due to the repulsion between adjacent streamlines, reducing the effective radius of the current sheets. This phenomenon is known as the *proximity effect*. Therefore, the distribution of RF current lines in a conductor (and the accompanying magnetic field) depends on both effects. Consequently, the calculation of inductance is a very specialized topic, which in each particular application is solved computationally and/or through approximations.

Some numerical methods and approximate formulas were developed more than a century ago, and we can cite the Japanese physicist Hantaro Nagaoka who published in 1909 a work on the calculation of inductances **[1]**. However, Nagaoka uses overly specialized mathematical elements (such as elliptic integrals, series expansions, and double and triple integrals). Another notable work is the classic and encyclopedic book *Inductance Calculations, Working Formulas and Tables* **[2]**. This volume considers the calculation of self-inductances and mutual inductances in many situations of practical interest. In any case, this work remains relatively advanced and impractical for radio amateurs and many engineers, mainly because some inductance formulas are presented with coefficients whose values are found in tables. Because of this, some manufacturers of magnetic cores experimentally determine the value of the inductance factor:

$$A_L \equiv \mu G$$

of the cores they manufacture. This factor, which includes the material (μ_{rel}) and the geometry (G), is reported in the datasheets, so that the designer can calculate the inductance simply with:

$$L = A_L N^2$$

It is common for manufacturers to experimentally determine this factor using:

$$A_L = \frac{L_{100}}{10\,000}$$

where L_{100} is the inductance measured directly with a coil of N=100 turns on the core. Strictly speaking, for a given core, the factors A_L corresponding to different numbers N of turns are only approximately equal, since the different coils occupy a different place in space. It should also be noted that some manufacturers specify *inductance factor* A_L but place the value of L_{100}.

Part II – CALCULATION OF SOLENOIDS AND TOROIDS

As explained in the previous part, the calculation of inductance is, in general, a very specialized job that is carried out

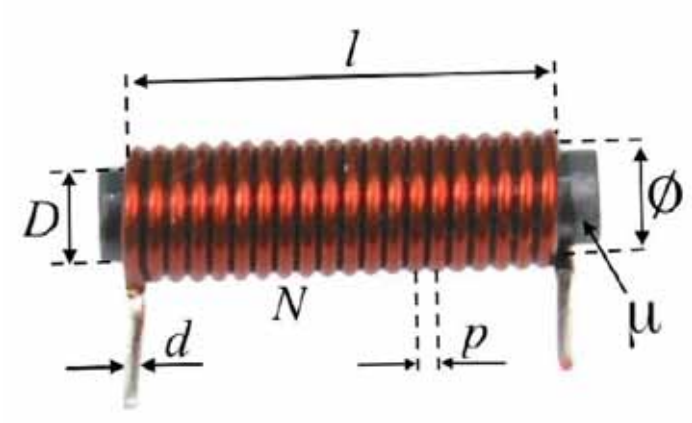

Figure 1 – Definition of the parameters of a simple solenoid.

with numerical methods. In many common cases in amateur radio, in which great accuracy is not required, the inductance L of a coil of N turns on a magnetic core is determined approximately with $L = A_L N^2$, where the inductance factor A_L is supplied by the magnetic core manufacturer. However, in many situations, the coil does not have magnetic material inside, or if it does, A_L is simply not known. Therefore, it is necessary to have a practical way to calculate L in any situation.

Among the coils most used by radio amateurs are the cylindrical ones (*solenoids*) and the annular ones (*toroids*), with a single layer of turns. Therefore, in this work we first show the approximate formulas to calculate the inductance of a solenoid, which are implemented in calculators freely available on the internet. Then, as an example, the inductance value obtained using the formulas and two calculators is compared, and another example shows the calculation of the number of turns in the design of a loading coil in just 4 simple steps, derived from the development of the approximate formulas. Subsequently, from the expression for a very long solenoid, the corresponding expressions for the toroidal coil are derived, with which the magnetic permeability of the core material can be found experimentally. Maintaining conceptual rigor, everything is presented with understandable language, easy-to-use formulas and the calculations can be performed in a couple of minutes with a simple pocket calculator.

Simple solenoid

The *simplest* cylindrical coil (the one designed with the smallest number of parameters) is built with a layer of enameled wire of diameter d (with negligible varnish thickness). The wire is wound on a support of diameter D, which can be a cylindrical PVC tube or the magnetic core itself (see **Figure 1**). Then the **effective diameter** $\emptyset$ and the **effective area** A_E of the solenoid are estimated with:

$$\emptyset = D + d \qquad \textbf{Equation 6}$$

$$A_E = \tfrac{\pi}{4}\emptyset^2 \qquad \textbf{Equation 7}$$

In practice, when there is a magnetic core, most of the field lines are concentrated in the material, and then the effective area value may be a little less than the A_E value determined with $\emptyset$. This difference is not very significant when the core occupies the entire interior of the turns, but in any case, these corrections, which are intended to calculate L more accurately, are not usually important or necessary in the field of amateur radio (where operating frequency varies along a band).

In general, in a uniformly wound solenoid, the separation p (*pitch*) of the centers of the turns is a distance equal to or greater than d. Then, the length of the solenoid is estimated with:

$$l = Np \quad (p \geq d) \qquad \textbf{Equation 8}$$

The relationship between length and diameter allows the different types of cylindrical coils to be classified:

- $l < \emptyset$: short
- $l = \emptyset$: "square" (square profile)
- $l > \emptyset$: long
- $l \gg \emptyset$: very long

Infinitely long cylindrical coils are the limit of the last type ("very long"). In this work we consider the simplest solenoid, with compact winding ($p = d$) and whose inductance is determined only by four parameters: μ_{rel}, N, $\emptyset$ and l, or μ_{rel}, N, D and d.

Infinite solenoid

By their nature, the magnetic field lines are always closed, and in very long solenoids the field is approximately uniform in most of the central turns, and practically zero in the central outer part near the winding (see **Figure 2).**

Therefore, long and very long solenoids have an inductance of the same order of magnitude as the inductance L_∞ of an infinitely long solenoid. It is easy to show that the geometric factor of this solenoid is: $G_\infty = A_E/l$, and then,

$$L_\infty = \mu_{rel}\mu_0 \frac{A_E}{L} N^2$$

Then, with **Equation 5**: l_∞ is expressed in microhenries:

$$L_\infty(\mu\text{H}) = \mu_{rel} \frac{2\pi}{5} \frac{A_E}{l} N^2 \frac{\mu\text{H}}{\text{m}}$$

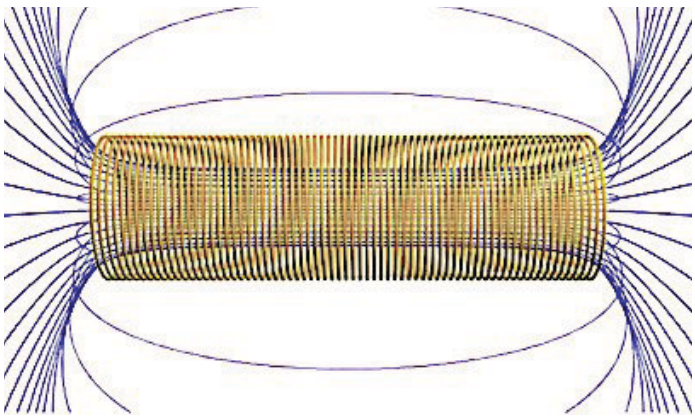

Figure 2 – Magnetic field lines in an elongated simple solenoid.

Finally, using **Equation 7**:

$$L_\infty(\mu\mathrm{H}) = \mu_{rel}\frac{(\pi\emptyset N)^2}{10l}\frac{\mu\mathrm{H}}{\mathrm{m}} \qquad \textbf{Equation 9a}$$

In practice, no solenoid is infinite. Therefore, **Equation 9a** represents the inductance value that increasingly longer solenoids approach, given that they have the same diameter (∅) and the same ratio of turns per unit length (N/l).

It should be noted that due to the proportionality of the length with the number of turns given in **Equation 8**, the expression for the inductance of the infinite solenoid can also be written in the form:

$$L_\infty(\mu\mathrm{H}) = \mu_{rel}\frac{(\pi\emptyset)^2 N}{10\times p}\frac{\mu\mathrm{H}}{\mathrm{m}} \quad (p \geq d) \qquad \textbf{Equation 9b}$$

This last expression is very useful in the design of solenoids because from the approximate value of L_∞, the number of turns can be estimated.

Approximate formulas

The value of the inductance *L* of any solenoid calculated numerically is usually expressed as a correction to the inductance of the infinite solenoid:

$$L = L_\infty k_L \qquad \textbf{Equation 10}$$

where k_L is a dimensionless factor (which will depend on ∅ and *l*) known as the **Nagaoka coefficient**. This coefficient tends to 1 as the coil becomes longer. Since it is now possible to calculate k_L computationally with great accuracy, it might seem that it is no longer necessary to look for approximate formulas. However, approximations are still very useful and important in several ways. They can be used to derive simple analytical expressions applicable in particular cases. Some technicians and radio amateurs also prefer to do the calculations by evaluating a formula with a calculator or by programming it. Therefore, it is useful to have formulas that are relatively simple without having to look up the value of coefficients in tables.

Among the notable works, we can mention the work of Richard Lundin published in 1985.**[3]** What is known as *Lundin's Handbook Formula* are two expressions of remarkable accuracy, one for short and "square" coils ($l \leq \emptyset$) with error less than 0.0002%, and another for long coils ($l > \emptyset$) with error less than 0.0003%.

In amateur radio and engineering, the approximate formula that is probably the most used is *Wheeler's formula* for solenoids of length equal to or greater than 40% of the diameter ($l \geq 0.4\emptyset$).**[4]** This formula, apparently derived in 1925, was published in 1928 by Harold Alden Wheeler (1903–1996), an American physicist and electrical engineer noted for mathematics, antennas, radio circuits, and microwaves. Many calculators on internet pages have this relationship programmed because it is simple, has a single empirical coefficient, has a very small inaccuracy (±0.33%), and only excludes solenoids that are too short. It could be slightly refined using the following equation [**5**]:

$$k_L = \frac{1}{1+0.4502\,\emptyset/l} \quad \text{for} \quad l \geq 0.4\,\emptyset \;\; (\pm 0.32\%)$$

then, with this value of k_L and the Equation 9a in **Equation 10**, and arranging terms, we have the equation that we will call "Optimized Wheeler's 1928 restricted formula":

$$L(\mu\mathrm{H}) = \frac{\mu_{rel}(\pi\emptyset N)^2}{10\;l+4.502\;\emptyset}\frac{\mu\mathrm{H}}{\mathrm{m}}\;(\pm 0.32\%)\;\text{for}\; l \geq 0.4\,\emptyset \qquad \textbf{Equation 11}$$

It is interesting to note that after 54 years, Wheeler published a short paper with a couple of approximate formulas for solenoids of any length/diameter ratio, [6] paying the price of increasing the inaccuracy and adding more empirical coefficients. In the work he uses the degree of elongation (or *form factor*) of the simple solenoid, which is given by the relationship between the length and the semi-perimeter ($\pi\,\emptyset/2$):

$$z \equiv \frac{2l}{\pi\emptyset} \qquad \textbf{Equation 12}$$

One of the formulas has three coefficients and an inaccuracy of 0.91%, but it can be improved [5] with an expression that, after rearranging terms, is:

$$k_L = z\left[\frac{2.666}{1+2.9484z} + \ln\left(\frac{0.10250}{z}\right)\right]\;(\pm 0.7\%) \qquad \textbf{Equation 13}$$

Then, with **Equations 9a**, **12** and **13** in Equation 10, after rearranging, we finally have the expression that we will call the *Optimized Wheeler's 1928 unrestricted formula*:

$$L(\mu\mathrm{H}) = \mu_{rel}\emptyset N^2\frac{\pi}{5}\left[\frac{2.666}{1+2.948438z} + \ln\left(\frac{0.102496}{z}\right)\right]\frac{\mu\mathrm{H}}{\mathrm{m}} \quad (\pm 0.7\%) \qquad \textbf{Equation 14}$$

It is observed that if the same relationship *l*/∅ is maintained (*z* constant), the inductance (which is always proportional to $\mu_{rel}N^2$) is proportional to the diameter ∅. It should be noted that the natural logarithm is the only operation that requires the calculator to be *scientific*. The other operations are elementary, and the calculation of **Equation 14** can be done in a couple of minutes with the simplest pocket scientific calculators that cost less than 20 USD. Any way, most cases correspond to $l \geq 0.4\,\emptyset$, and for **Equation 11**, any calculator is suitable.

Example 1

Below, the results of calculating the inductance of a typical coil are compared, obtained by the two approximate formulas and by two calculators available on the internet. The coil has an air core μ_{rel}=1, it is compactly wound ($p = d$) on a PVC tube with external diameter *D*=32 mm, with *N*=30 turns of enameled copper wire of intermediate diameter: d=0.6 mm (used in some applications up to 100 W). Then, using **Equations 6** and **8**,

$$\emptyset = D + d = 0.0326\,\mathrm{m}$$

$$l = Nd = 0.018\,\mathrm{m}$$

Method 1: Using the restricted formula.

Since $l \geq 0.4\,\emptyset$, we use Equation 11:

$$L_1(\mu\text{H}) = 1\frac{(\pi\times 32.6\times 10^{-3}\text{m}\times 30)^2}{(10\times 18+4.502\times 32.6)\times 10^{-3}\text{m}}\frac{\mu\text{H}}{\text{m}} \approx 28.890\ \mu\text{H}$$

To compare the following values, L_1 is adopted as a reference, as it has the least inaccuracy (0.32%).

Method 2: Using the unrestricted formula.

To calculate the inductance $L_2(\mu\text{H})$ with Equation 14, first the shape factor and the two factors are calculated:

$$z \equiv \frac{2l}{\pi\emptyset} \approx 0.351508$$

$$\mu_{rel}\emptyset N^2\frac{\pi}{5} \approx 18.4349$$

$$\frac{2.666}{1+2.94838\,z} + \ln\left(1+\frac{0.102496}{z}\right) \approx 1.56506$$

therefore,

$$L_2 \approx 28.85173\,\mu\text{H}$$

Regarding the value L_1, the value L_2 has a percentage discrepancy:

$$\frac{L_2-L_1}{L_1}\times 100 = \frac{28.85173-28.890}{28.890}\times 100 \approx -0.1\,\%$$

Method 3: Using the "Air Cored Inductor Calculator"[7]

With $\emptyset$=32.6 mm, l=18 mm and N=30, $L_3 \cong 28.822\,\mu\text{H}$ is obtained, whose percentage discrepancy with respect to L_1 is $\approx -0.2\,\%$.

Method 4: Using the "Coil Inductance Calculator" [8]

With "Single-Layer, air coil", N=30 and with $\emptyset$ and l in centimeters, $L_4 \cong 28.8\,\mu\text{H}$ is obtained, whose discrepancy with respect to L_1 is $\approx -0.3\,\%$.

Therefore, as the three discrepancies stay at absolute values less than 0.35%, the values obtained with the unrestricted approximation and with the two calculators are equally acceptable as the first, whose accuracy is within 0.32%. In other words, the 4 results are practically equal and highly accurate.

Knowledge of the approximate formulas allows you to quickly calculate the value of the inductance with a certain accuracy using a simple calculator or spreadsheet (without using the web). On the other hand, if you want to use a calculator available on the internet, the approximate formulas allow you to make a preliminary verification calculation to see if the chosen calculator is working correctly (the discrepancy should be less than 0.35%).

Example 2

Loading coil design in 4 simple steps

This example shows the convenience of knowing the context of the approximate formulas, and not just the final equations. Suppose that in a backyard there is a half-wavelength *end-fed* antenna (EFHW) for the 40 m band (7.0–7.3 MHz) built with wire almost 20 m (66 ft.) long. It is desired to extend its operation to the 80 m band (3.50–3.75 MHz), but since the necessary space is not available, it was decided to add a little more wire attached to the 20 m with a loading coil, which must be designed and build. This coil has two functions. On the one hand, it allows the antenna to resonate at 80 m with a shorter length, and on the other hand, it acts as a low-pass filter for the 40 m band, in which the transmitter should only "see" the 20 m wire in length that reaches the coil. The design is very simple, and consists of the following four steps, to find a satisfactory value of *N*.

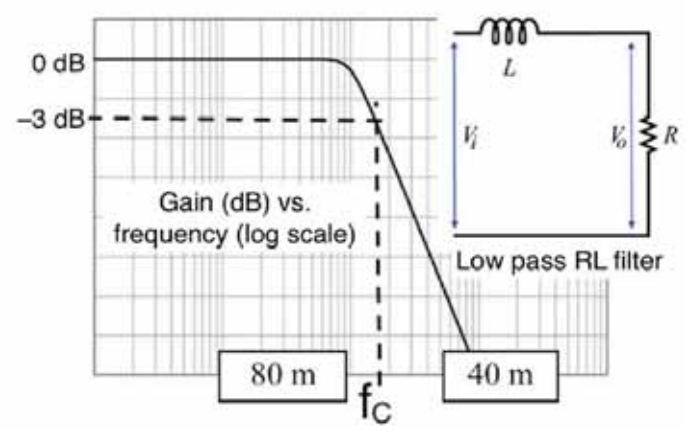

Figure 3 – Schematic diagram of the gain (in dB) of the RL low-pass filter versus frequency (on a logarithmic scale). The cut-off frequency is observed between the 80 and 40 meter bands.

Step 1: You can start with a PVC pipe and a roll of enameled wire, so the parameters *D* and *d*, and consequently the diameter $\emptyset$ would be defined. Suppose that the outer diameter of the tube is 1+1/4" (32 mm) and that the wire size is AWG 18 (diameter 1.0 mm). Then, *D*=0.032 m, *d*=0.001 m and:

$$\emptyset = 0.033\ \text{m}$$

Step 2: Next, the inductance *L* of the coil is calculated. For this, it is necessary to know: (a) the resistance *R* of the load represented by the antenna and (b) the cut-off frequency f_c (which corresponds to –3 dB, an attenuation of half the power). It is easy to see that for a *passive RL low-pass filter* the cutoff frequency is (see **Figure 3**):

$$f_c = \frac{R}{2\pi L} \qquad \textbf{Equation 15}$$

The *R*-value of the load represented by the antenna impedance can vary significantly (due to height, type of wire, way of placement, etc.). Therefore, the design needs to be robust enough so that in the worst case, the frequency, f_c, stays between the adjacent extremes of the bands. Suppose that *R* is between 2 kΩ and 3 kΩ, that is, *R*=(2.5±0.5) kΩ, or *R*=2.5 kΩ (±20%). Then, you choose:

$$f_c = 5\ \text{MHz}$$

because even with a ±25% variation, the cutoff frequency stays between 3.75 and 7 MHz. So,

$$L(\mu\text{H}) = \frac{R}{2\pi f_c(\text{MHz})} = \frac{2500\Omega}{2\pi\times 5\ \text{MHz}} \approx 79.6\ \mu\text{H}$$

Step 3: To determine the L_∞ value of the inductance of the corresponding infinite solenoid we must estimate the Nagaoka

coefficient from Equation 10. We assume that our solenoid will be long, and then we test with an initial value of k_L of 85%, that is:

$$L_\infty(\mu\text{H}) = L(\mu\text{H})/k_L = 79.6\mu\text{H}/0.85 = 93.6\ \mu\text{H}$$

Step 4: If the solenoid has an air core it is $\mu_{rel} = 1$. Then, using **Equation 9b** and assuming compact winding ($p = d$):

$$N = \frac{10\times L_\infty(\mu\text{H})d}{\mu_{rel}(\pi\emptyset)^2}\frac{\text{m}}{\mu\text{H}} \approx 87.1$$

Therefore, it is adopted that:

$$N \equiv 87$$

and then, using Equation 8 we get:

$$l = Nd = 0.087\ \text{m}$$

When $l < \emptyset$, we must continue with the unrestricted formula given by Equation 14, but since $l \geq \emptyset$ is verified here, Equation 11:

$$L(\mu\text{H}) = \frac{\mu_{rel}(\pi\emptyset N)^2}{10l+4.502\emptyset}\frac{\mu\text{H}}{\text{m}} \approx 79.9\mu\text{H}$$

Generally, this value of L is different than the originally searched value. Therefore, you must always verify the corresponding cut-off frequency value:

$$f_c(\text{MHz}) = \frac{R}{2\pi L(\mu\text{H})} = \frac{2500\Omega}{2\pi\times 79.9\mu\text{H}} \approx 4.98\ \text{MHz}$$

When the result is not satisfactory, we must proceed by trial and error. An excessive value of f_c is corrected by decreasing k_L (to increase L_∞, N and L, and thus decrease f_c). However, it is sufficient to directly increase N to recalculate l, L and f_c, to check whether the new value of f_c is suitable or requires another iteration. In general, one or two iterations is sufficient.

Toroidal coil

A type of magnetic core widely used by radio amateurs is *toroidal* cores. They are *annular* (ring-shaped) cores because it is easier to cut a "slice" from a cylindrical tube than to make a toroid (which is why they have a rectangular cross section instead of circular (see **Figure 4).**

Figure 4 – Annular coil (left) and toroidal coil (right).

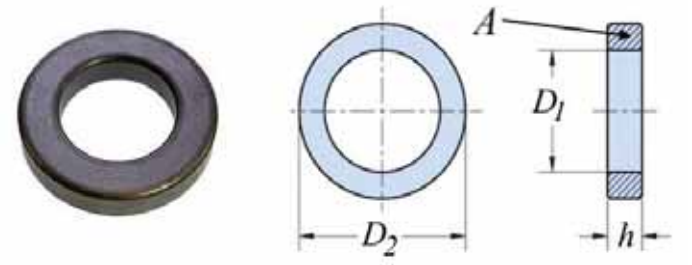

Figure 5 – Annular core dimensions.

To begin the calculations, the annular core is assumed to be *thin* toroidal, that is, the cross-sectional diameter is assumed to be considerably smaller than the inner diameter of the torus. Additionally, a core made of high-permeability material, such as ferrite, is considered more effective than one made of iron powder. This makes the calculation very simple, since the field inside the core can be considered uniform along the perimeter, then the inductance, L_T, of the toroidal coil is calculated as the inductance of an infinite solenoid: $L_T = \mu G_\infty N^2$,where $G_\infty = A_E/l$. To make these calculations, the dimensions of the annular geometry are used: inner diameter D_1, outer diameter D_2 and height h. Therefore, the cross-sectional area of the core is $A = h(D_2 - D_1)/2$ (see **Figure 5).** If the relative magnetic permeability of the core material is, $\mu_{rel} \gg 1$, the magnetic field lines are more concentrated in the material, and the effective cross section A_E of the coil wound closely on the annular core is practically equal to A.

On the other hand, to calculate the inductance, L_T, of the annular coil, the geometric factor (A_E/l) of an infinite solenoid is expressed with the average perimeter of the annular core,
$l = \pi\overline{D}$, calculated with the average diameter $\overline{D} = (D_2 + D_1)/2$, i.e.:

$$G_\infty = \frac{A_E}{l} = \frac{A}{\pi\overline{D}} = \left(\frac{D_2-D_1}{D_2+D_1}\right)\frac{h}{\pi}$$

Therefore,

$$L_T = \mu_{rel}\mu_0 G_\infty N^2 = \mu_{rel}\mu_0\left(\frac{D_2-D_1}{D_2+D_1}\right)\frac{h}{\pi}N^2$$

Then, expressing h in millimeters, μ_0 in μH/mm and regrouping terms results in:

$$L_T(\mu\text{H}) = \mu_{rel}\left(\frac{D_2-D_1}{D_2+D_1}\right)h(\text{mm})\left(\frac{N}{50}\right)^2\frac{\mu\text{H}}{\text{mm}}$$

Equation 16

The diameters D_1 and D_2 can be expressed in any unit, as long as they are the same in the subtraction as in the addition.

Permeability measurement

Equation 16 shows that for the toroidal core the inductance factor is:

$$A_L(\mu\text{H}) = \frac{L_T(\mu\text{H})}{N^2} = \mu_{rel}\left(\frac{D_2-D_1}{D_2+D_1}\right)\frac{h(\text{mm})}{2500}\frac{\mu\text{H}}{\text{mm}}$$

For example, from the Fair-Rite Catalog for the FT-240-43 toroidal ferrite core, there are the following nominal values: $\mu_{rel} = 800$, $D_1 = (35.55 \pm 0.85)$ mm, $D_2 = (61 \pm 1.30)$ mm, $h = (12.7 \pm 0.50)$ mm, and $A_L = 1075$ nH ($\pm 20\%$).**[9]** Replacing these data in the previous expression, $A_L(\mu\text{H}) \approx 1.069\mu\text{H}$ or 1069 nH, which has a discrepancy of less than 0.6% with respect to the nominal value of A_L given by the manufacturer. On the other hand, the value $\pm 20\%$ of the tolerance is almost entirely due to the dispersion in the value of μ_{rel}, since the tolerances for D_1 and D_2 are only 2% and for h, 4%. Therefore, when it is needed to know the magnetic permeability with a smaller dispersion, it will be necessary to measure μ_{rel} of the material of that particular core (instead of using the nominal value).

To experimentally determine μ_{rel}, Equation 16 is inverted:

$$\mu_{rel} = \left(\frac{50}{N}\right)^2 \frac{1}{h(\text{mm})} \left(\frac{D_2+D_1}{D_2-D_1}\right) L_T \ (\mu\text{H}) \qquad \textbf{Equation 17}$$

Relative permeability can be calculated by using different numbers of turns and directly measuring the inductance for each coil. For example, for N=5, 10, and 20, the numerical factors $\left(\frac{50}{N}\right)^2$ will be 100, 25, and 6.25 corresponding to the respective direct measurements $L_{N=5}(\mu\text{H})$, $L_{N=10}(\mu\text{H})$, and $L_{N=20}(\mu\text{H})$ of the inductances. Theoretically, assuming the same magnetic excitation due to the current of the measuring instrument, the results $\mu_{rel(N=5)}$, $\mu_{rel(N=10)}$, and $\mu_{rel(N=20)}$ obtained respectively with each value of N, should be equal (within the experimental errors), since μ_{rel} is a property of the material. However, depending on how the wire was wound on the core, there could be a larger difference that is not due to the material, mainly with low permeability materials and due to windings with few turns. Therefore, to determine the relative magnetic permeability with lower experimental uncertainty, it is convenient, (a) to make several measurements with different numbers of turns, (b) that the values of N are as large as possible, and (c) that all the turns compactly wound on a fraction of the perimeter (On the contrary, on some internet sites you see measurements with a factor of 100, since only 5 turns are used, a single measurement is made and the wire is wound on uniformly around the entire of the perimeter. This experimental situation can lead to a very inaccurate result).

José Luis Giordano, CE4TW, is a physicist who has worked at the Balseiro Institute and Bariloche Atomic Centre in Argentina, the University of Zaragoza in Spain, and the University of Talca in Chile. Now retired from academic life, Luis lives in Chile and obtained his amateur radio license in 2021. He is the author of four books, several papers on physics, and articles in several ham radio magazines. Luis is especially interested in DX, HF and broadband transformers. He can be reached at ***JLGiordano@ hotmail.com****.*

References

[1] H. Nagaoka, "The inductance coefficients of solenoids," J. Coll. Sci., Tokyo, vol. 27, no. 6, pp. 18–33, 1909.

[2] F. W. Grover, Inductance Calculations: Working Formulas and Tables. New York, NY, USA: D. Van Nostrand Company, Inc., 1946.

[3] R. Lundin, "A handbook formula for the inductance of a single-layer circular coil," Proc. IEEE, vol. 73, no. 9, pp. 1428–1429, Sept. 1985. [Online]. Available: **http://ieeexplore.ieee.org/iel5/5/31353/01457572.pdf**

[4] H. A. Wheeler, "Simple inductance formulas for radio coils," Proc. IRE, vol. 16, no. 10, pp. 1398–1400, Oct. 1928.

[5] D. W. Knight, "An introduction to the art of solenoid inductance calculation with emphasis on radio-frequency applications," ver. 0.20 (unfinished), Feb. 4, 2016.

[6] H. A. Wheeler, "Inductance formulas for circular and square coils," Proc. IEEE (Letters), vol. 70, no. 12, pp. 1449–1450, Dec. 1982.

[7] J. Parfrey, "Air cored inductor calculator," M0UKD. [Online].

[8] "Coil inductance calculator," **66pacific.com**. [Online].

[9] "Fair-Rite components for the electronics industry," 17th ed., 2013, p. 106. [Online]

Stefan Scholl, DC9ST
Achtmorgenweg 24 53343 Wachtberg, Germany | **dc9st@panoradio-sdr.de**

Automatic Identification of Shortwave Signals with Neural Networks

Neural networks, a core tool of modern machine learning, are now being applied to radio spectrum analysis. This article shows how a deep convolutional neural network can classify more than 160 shortwave signal modes from just one second of data.

Introduction

Everybody who has looked and listened into the shortwave band probably knows the situation: There are a multitude of different analog and digital signals with different sounds and shapes in the waterfall as shown in **Figure 1**. Often it is hard to identify these signals in terms of their transmission mode, especially considering the large variety of digital signals. This article presents an approach to the automatic identification of radio signals with computer algorithms based on neural networks.

Automatic signal identification or classification is the task of determining the type (or mode) of a radio signal automatically using a computer algorithm. This can be useful for several purposes, such as spectrum monitoring and surveillance, the support of dynamic spectrum access in cognitive radios, or for the identification of digital transmission modes in amateur radio.

The basic principle of automatic signal identification is depicted in **Figure 2**. It consists of a classifier, which inputs a signal and after some calculations outputs the present signal type as one of the pre-defined output classes.

In this article, the classification algorithm is a deep neural network. Neural networks belong to the field of machine learning, a modern approach to pattern recognition, which is often summarized under the term artificial intelligence (AI). This neural network is specifically designed for the identification of 160 different shortwave signal modes, such as Morse code, single-sideband voice, PSK-31, or AM broadcast. It covers most of the modes present in the shortwave band. Although the focus is on shortwave here, the underlying principle also works for signals from other frequency bands, such as VHF or UHF.

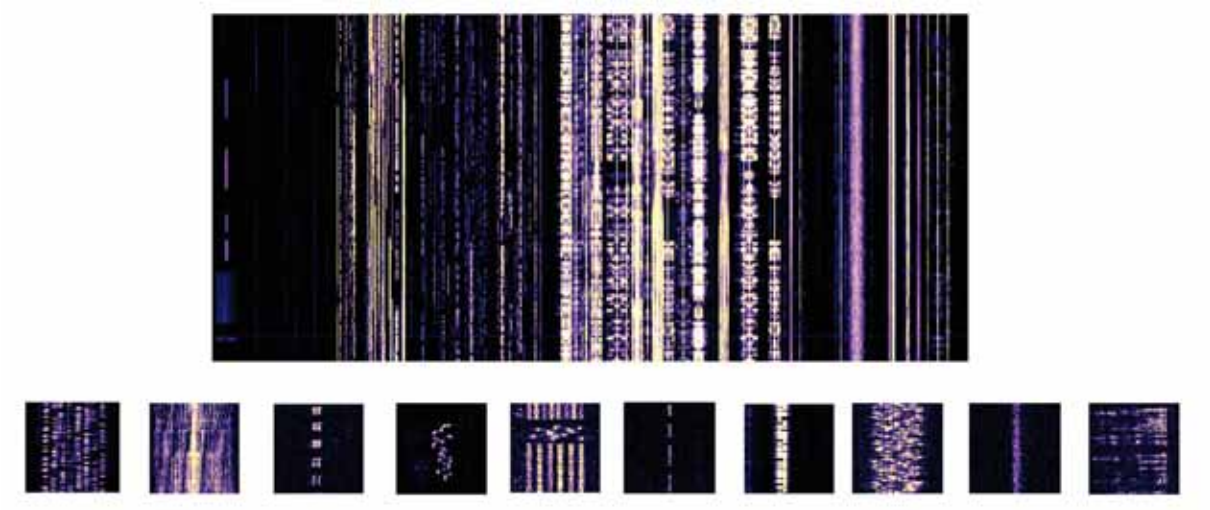

Figure 1 – A look into the shortwave band shows a multitude of different signals.

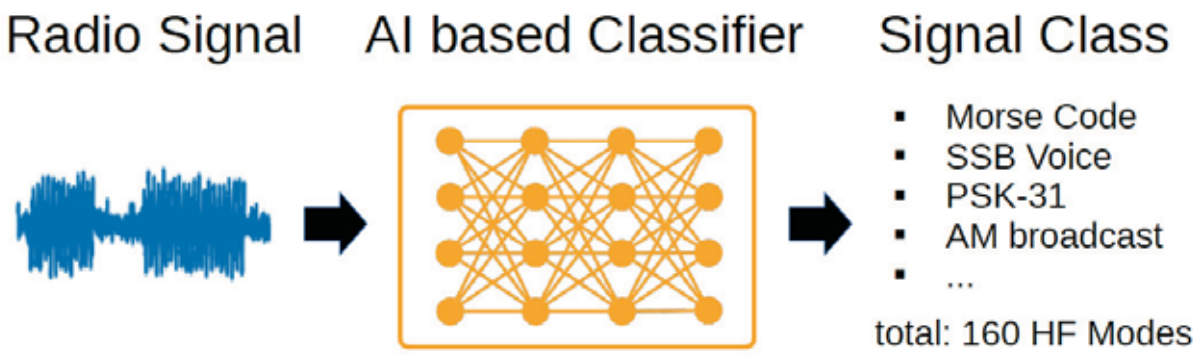

Figure 2 – The basic setting in signal identification.

Shortwave Signals

The shortwave band covers frequencies from approximately 3 to 30 MHz. Radio wave propagation in this frequency range has some interesting properties: Shortwave radio waves can be reflected by the ionosphere back to Earth. Therefore, beyond line-of-sight communication over thousands of kilometers is easily possible. In addition, little equipment is required to set up long distance communications – often a compact transceiver and a decent antenna installation is sufficient. Furthermore, shortwave communication is independent from large-scale infrastructure such as satellites, sea cables and hard to block by third parties.

Due to these advantages, many operators are using shortwave signals for communication. Some typical users of the shortwave bands are:

- Broadcasting (e.g., AM or DRM)
- Amateur radio (wide variety of analog and digital modes)
- Aviation (e.g., long-range aircraft communications, HFDL)
- Weather services (e.g., WEFAX, RTTY weather data)
- Embassies
- Intelligence, military and security authorities
- Radar (civil and military) and ionosondes

Because of potentially worldwide coverage, a single radio can receive many different signals and modes from all over the world. The number of different shortwave modes probably goes into the hundreds, while not all of them are documented or even well-known. In addition, a large fraction of the documented modes may be outdated and no longer used. The well-known signal database Sigidwiki **[2]** lists over 220 different shortwave signal types. A similar number of modes is documented in Roland Proesch's *Technical Handbook for Radio Monitoring* **[3]**. From my own experience roughly 100 shortwave signal types are used on a regular basis in the shortwave band **[1]**.

Machine Learning

Before considering signal identification in detail, an introduction to the basic ideas of neural networks and machine learning is presented.

A Brief Introduction to Machine Learning

Although the ideas of neural networks and machine learning go back to the 1940s, only since around 2010 has a huge interest in machine learning techniques started. In recent years machine learning has experienced great advances that have led to impressive achievements in many applications. Well-known examples are object detection in image processing or automatic language translation systems, such as Google Translate. More recently systems like ChatGPT **[4]** demonstrated the power of AI to a broad range of people.

Machine learning in principle is algorithms that are good in detecting complex patterns in data. This is useful for detecting objects in images, linguistic patterns in languages or any other patterns in further applications. Accordingly, machine learning can also be applied to radio signals to detect patterns that are useful to distinguish different signal modes. Therefore, it is worth considering machine learning techniques to enable automatic signal identification.

Before we proceed with the design of a classifier for shortwave signals, a more detailed view on machine learning and how it is different from classical algorithm design is given.

Classical Algorithms vs Machine Learning

The machine learning approach works fundamentally different from classical, i.e., non-machine learning, algorithm design. To clarify the difference, we can consider the simple example task of designing an algorithm to detect AM modulation in radio signals.

Classical algorithm design

An algorithm designer, who is an expert in the field of radio signal recognition, takes a close look at the signal to identify signal properties, which are characteristic for AM signals. These characteristic properties, also called features, should be unique to AM signals. Some exemplary characteristic features could be derived from the spectrum of an AM signal, e.g.:

- A clear peak in the center (originating from the carrier)
- Symmetry of spectrum around the carrier

After the selection of these two characteristic properties, the designer creates an algorithm that detects the clear peak in

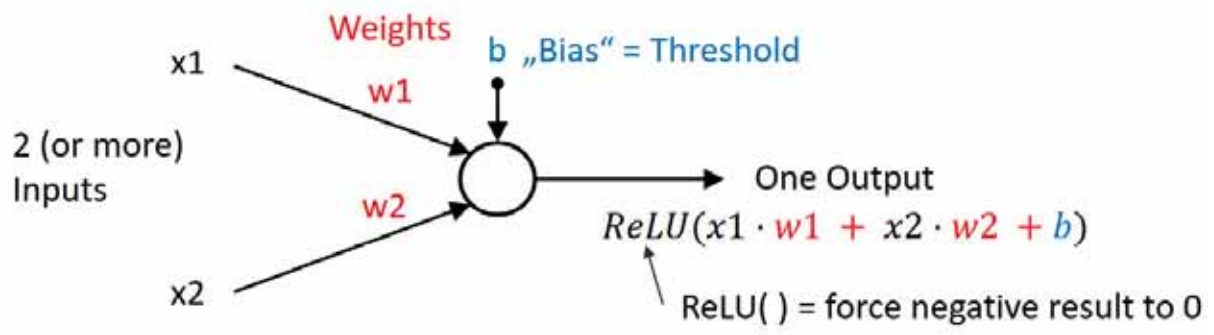

Figure 3 – A simple single neuron with two inputs.

the spectrum and checks for spectral symmetry. Typically, this involves some manually tuned acceptance thresholds, which determines when the peak and symmetry requirements are fulfilled. Only if the two characteristic properties are present is the signal declared as an AM signal.

This "classical" method may provide decent results on most signals. However, in practice the pre-defined features may not always be a good choice. For example, the AM signal's spectrum may not be symmetric when frequency fading is present. In addition, the process of designing characteristic features by hand for each signal class is expensive if there is a large number of signal types to be detected, because they have to be unique among all classes. Especially for some analog signals, finding characteristic features can be difficult.

Since some of these issues can be tackled by the approach of machine learning, it is worth considering this alternative approach.

Machine Learning

The main difference between classic algorithm design and machine learning is the way the characteristic signal properties are selected. In classical algorithm design the characteristics are selected by an expert after close signal inspection. On the other hand, machine learning uses a large amount of example signals of AM and non-AM signals to train a neural network. During training, the network is tuned step-by-step to make it calculate the correct output class (here: *AM* or *Non-AM*). After training, the neural network has automatically learned to calculate characteristic properties for each of the signal classes without the need of manual intervention. The learned characteristics are encoded in the network and are typically more abstract than manually designed features. Thus, they are harder to interpret as physical signal properties.

Although machine learning is the more recent approach, there are also drawbacks that need to be considered, e.g., the need for substantial amounts of example training data or the lack of interpretability of the neural network's operations and selected features.

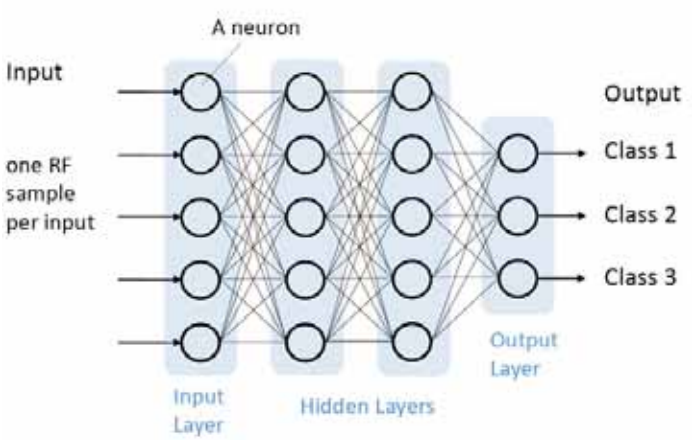

Figure 4 – A typical neural network consists of many neurons arranged in multiple layers.

Neural Networks in Detail

Neural networks are probably the most widely used machine learning algorithms for pattern recognition. They were originally designed many decades ago to mimic the function of the human brain, although today this analogy is considered outdated. Neural networks mainly consist of many neurons, which are arranged in multiple layers.

A single neuron implements a remarkably simple function and has two or more inputs and one output. A simple neuron is depicted in **Figure 3**:

$$y = \text{Output Function}\ (w_0 \times x_0 + w_1 \times x_1 + w_2 \times x_2 + b)$$

Each input x is multiplied by a weight value w, then summed up together with a "bias" value b. The output function is often a rectified linear unit (ReLU) functionality, which is simply a clipping operation at 0, i.e., it forces negative output values to 0. The weights w and bias b are called the *parameters* and are most important, because they define the function of the neuron. The values of the weights and biases are determined during the training of the neural network and fixed afterwards.

Although a single neuron is not very powerful, multiple neurons can be arranged in parallel to form a layer, which can process a vector of data, such as a radio signal. A simple example of a neural network with multiple layers in shown in **Figure 4**. Modern neural networks typically stack many of these layers and are therefore called *deep* neural networks. Deep neural networks are considered as the most powerful machine learning techniques today.

When arranging multiple neurons in a layer, several structures are possible. Commonly used processing types of layers are depicted in **Figure 5**:

- Fully Connected Layer: Each neuron is connected to every input value. This creates a densely connected layer, where each neuron has a lot of parameters. Fully connected layers are often found as the last layers in a neural network.
- Convolutional Layer: This layer basically implements a convolution operation. Thus, it works like a digital FIR filter, where the neuron's weight works as the filter coefficients. Because of the non-linear output function in the neuron, the filters are typically not linear. The filter coefficients are not predefined but are learned during training.
- Pooling Layers: This layer reduces the length of the input by combining two values into a single one by simply outputting the larger of the two input values. When processing RF signals this operation is similar to decimation and results in a shorter signal. Strictly speaking, pooling layers do not contain any neurons rather than simple max operations and do not have any learnable parameters.

In machine learning, so-called *convolutional neural networks* (CNN) are widely used in many applications, which combine the type of layers from Figure 5. A typical structure of a CNN are several stacked convolutional and pooling layers. With one or more fully connected layers at the end. The last layer extracts the classification output.

Figure 6 sketches a simple CNN and the processing flow of an input signal. The input passes through several processing layers. Each layer progressively modifies the signal to extract characteristic features and properties by filtering. In the final, fully connected layer, the network selects the most likely output class.

Identification of RF Signals with Deep Learning

Basic Task

The classifier presented in this article takes a short portion of a radio signal with 4096 IQ samples as input. For a sampling frequency of 4 kHz this results in a bandwidth of 4 kHz and a signal duration of approximately one second. For each one second portion, a classification result is output.

The classifier covers the 160 signal modes shown in **Table 1**, ranging from ham radio, aviation and diplomatic, to military applications from various parts of the world. This covers a large fraction of the signals present in the shortwave spectrum.

Training Data

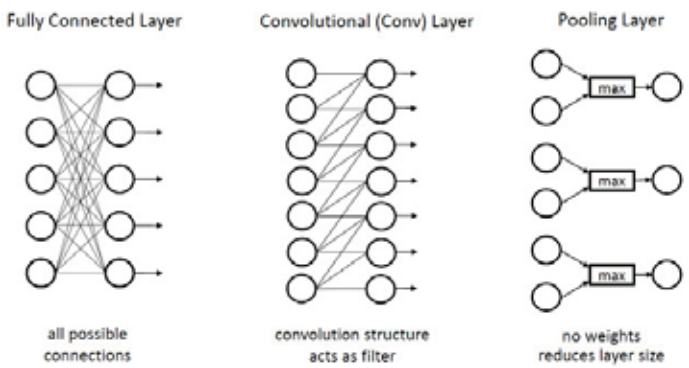

Figure 5 – Different layer types in a neural network.

The machine learning approach requires substantial amounts of example data for each of the considered signal modes for the training of the neural network.

The training data is based on synthetic and high-quality real-world signals from various open sources, such as Sigidwiki and others, including recordings and software generated signals. Especially in ham radio, free software tools (Fldigi, MultiPSK, etc.) are available to generate signals for training. For other signal types, such as SSB, AM or over-the-horizon-radars, simple custom generation software can be developed. For signal types, where no documentation is available, recordings from the bands can be used.

Until now, the training data is mostly software generated and "clean," with no distortions or real-world impairments like noise, frequency offsets or fading. A neural network trained on this clean data only would quickly be confused when faced with real-world signals, which can exhibit a large variety of distortions and impairments. Therefore, the training data is artificially distorted via software to make the network learn to ignore distortions and impairments that are irrelevant for signal identification.

Various distortions and impairments can occur in a communication system, some of which are depicted in **Figure 7**. Accordingly, the training data for this article has undergone the following artificial impairments:

- Random frequency offset between +/-500 Hz
- Random phase shift
- Random sample rate offset 0 to 1 %.
- Random SNR between -10 and +25 dB (Gaussian noise)
- Random introduction of impulsive noise to emulate QRN
- Bandwidth filter of random excess bandwidth
- Random channels: 16 Watterson fading models including CCIR-520 and ITU 1487 **[5]**

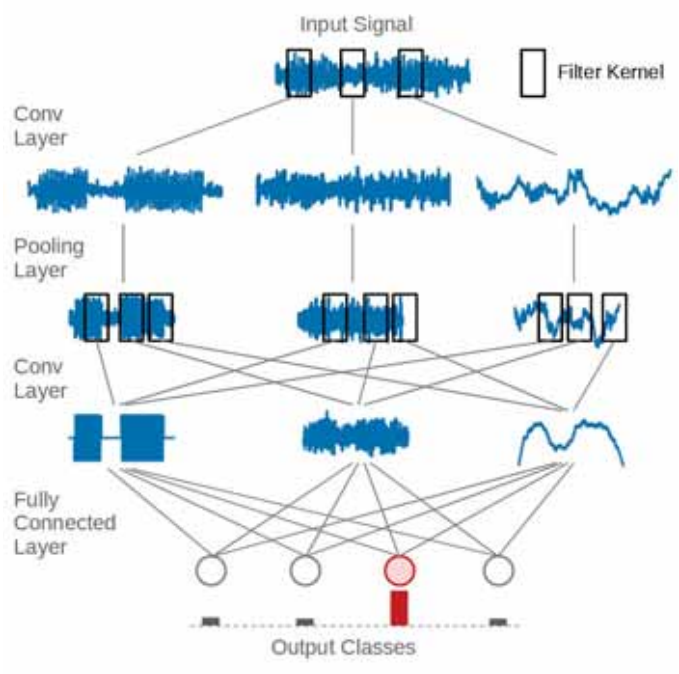

Figure 6 – Principle of signal processing in a neural network.

2G ALE	Codan Chirp Mode	Mahovik	Pol Intel FSK	Single-Sideband Audio (LSB)
3G ALE	Codan Selcall	Mazielka	Pol Intel FSK F03I	Single-Sideband Audio (USB)
ALE-400	Contestia 16/250	MFSK 11	Pol Intel QPSK	SSTV Martin 1
ALIS	DominoEx 11	MFSK 16	PSK 10	SSTV Martin 2
ALIS-2	DominoEx 16	MFSK 32	PSK 125	SSTV Robot 36
AM signal	DominoEx 22	MFSK 64	PSK 220F	SSTV Robot 72
ARQ-E(E3)	DominoEx 4	MFSK 8	PSK 250	SSTV Scottie 1
Chinese 4+4	DominoEx 5	MS-188-110A A16	PSK 31	SSTV Scottie 2
Chinese MIL Datalink 30	DominoEx 8	MS-188-110A B39	PSK 63	Stanag 4197
CIS-11	DPRK FSK	MS-188-110A serial	QPSK 125	Stanag 4285
CIS-112	D-Marker	Morse Code	QPSK 31	Stanag 4481 FSK
CIS-12	FSK 50/850	MT63-1000	QPSK 63	Stanag 4529
CIS-128	FT4	MT63-2000	RDFT	Stanag 4539
CIS-20	FT8	MT63-500	Robust Packet	T-Marker
CIS 200-1000	GMDSS-DSC HF	Nokia Adaptive MSG Terminal	POS-16	Thales Skyhopper
CIS-200-500	HC-265	Olivia 16/1000	POS-4	The Air Horn
CIS-3000	Hell 80	Olivia 4/125	ROS-8	The Alarm
CIS-36	Hell Feld	Olivia/Contestia 16/500	RTTY 100/450	The Buzzer
CIS-36-50 / CIS-50-50	Hell FSK	Olivia/Contestia 32/1000	RTTY 100/850	The Goose
CIS-45	HFDL	Olivia/Contestia 4/250	RTTY 45/170	The Pip
CIS-60	Iran Navy PSK modem	Olivia/Contestia 4/500	RTTY 50/170	The Squeaky Wheel
CIS-75-250	Iran Navy PSK modem v1	Olivia/Contestia 8/250	RTTY 50/425	Thor 11
CIS-8181	Iran Navy PSK modem v2	Olivia/Contestia 8/500	RTTY 50/450	Thor 16
CIS-93	Israel Navy Hybrid Preamble	OTH Radar	RTTY 75/170	Thor 22
CIS-MFSK-16 (XPA2)	Japan 32-Channel	Packet 300	RWM Time	Thor 8
CIS-MFSK-16 (XPB)	Japan 8-Channel	Pactor 1	Saab Grintek MHF-50	Throb 1
CIS-MFSK-20 (XPA)	Japan Slot Machine (idle)	Pactor 2	ICAO Selcal	Throb 2
CIS MFSK-68	Japan Slot Machine (TFC)	Pactor 3	Siemens CHX-200	Throb 4
Clover 2000	JT65	Pactor 4	Sine	Vara HF Std
Clover 2500	Link-11 CLEW	Pol Intel 4-FSK	Sitor A	Vara HF Narrow
Clover II	Link-11 SLEW / GM2100	Pol Intel BPSK P03k	Sitor B	Vezha-S
Codan	Link-22	Pol Intel BPSK P03i	Skyfax	Wefax

Table 1 – List of the supported modes originating from ham radio, aviation, military, diplomacy, and broadcasting.

For each example signal of 1 s duration, the impairments are randomly chosen. **Figure 8** shows some exemplary signals for the class "Morse code." It shows how various affects impact sections of Morse code signals. Easily visible are varying SNR, fading, and frequency offset.

The final training dataset consists of 7500 example signals per mode, resulting in a total of 1.2 million examples in the complete training dataset.

Training of a Neural Network

The neural network here is a CNN, which consists of an arrangement of 28 layers including convolutional, pooling and fully connected layers. The network successively processes the input radio signal following the basic principle shown in Figure 6. In total, the network has 1.7 million weights and bias parameters that need to be tuned during training.

For training, the data is fed into the network together with the information of the actual signal class of the data. Typically, it is necessary to train the network on the complete dataset many times to achieve convergence of the network parameters and good classification performance. This training process is often computationally expensive. Therefore, powerful GPUs are widely used, because their chipset architecture is well suited to the training algorithms.

After successful training, the parameters of neural network are fixed. Now the trained neural network is ready to input radio signals to identify them.

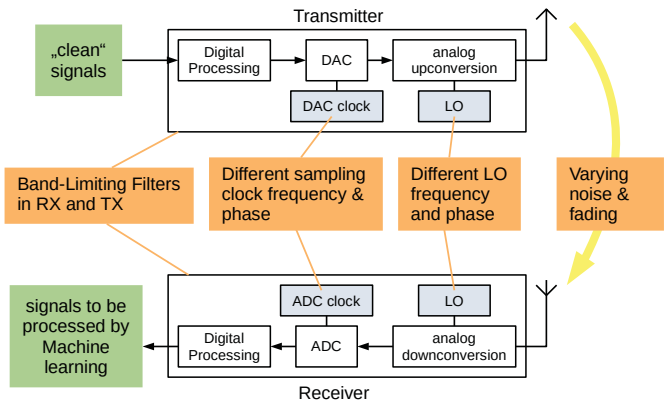

Figure 7 – Overview of the impairments a signal faces in a communication.

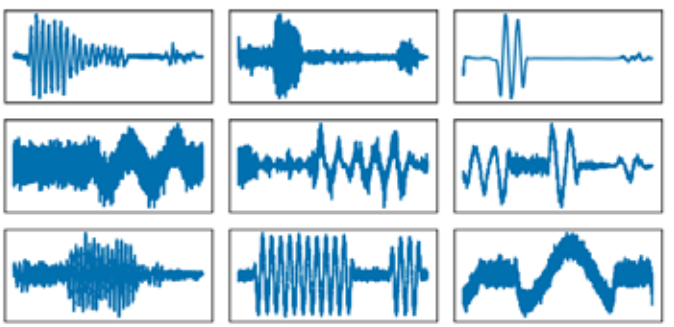

Figure 8 – Good training dataset for the class "Morse code" showing a high variation on different signal impairments, like noise, fading and frequency offsets.

Tested Modes	143 (most frequently occurring) out of 160
Receiver Hardware	Kiwi SDR, Airspy HF+, SDR Play, Twente WebSDR, Elad FDM-S3
Locations	Worldwide
Frequencies	3 - 30 MHz
Daytime and Season	All seasons and varying daytime
Signal SNR	-10 to 25 dB
Recording Duration	>35 hours total

Table 2 – Overview of the equipment, conditions, and properties used in the collection of the real-world test data

Real-World Test Data

For deployment and real-world operation, it is important to test the neural network on real-world data. For this purpose, an additional large test dataset of shortwave signals has been collected, that covers different real-world scenarios. The test data consists of actual recordings from different SDR receiver hardware at various locations, times, seasons, and operating frequencies. It includes different signal-to-noise ratios, fading channel conditions, as well as varying background noise from the environment in form of QRM and QRN. It should be noted that these signals are recorded "as they are" without any further processing, noise reduction, or frequency correction. These variations result in a highly diverse set of test data that allows for a meaningful measurement of accuracy in practical operation. An overview of the test data properties is shown in **Table 2.** The total amount of recorded signals sums to more than 35 hours. The test data also includes information on the signal-to-noise ratio of the recorded signals, allowing evaluation of accuracy versus SNR.

Classification Performance

To measure how well the trained neural network performs in practice, it is tested on real-world data. For that purpose, the

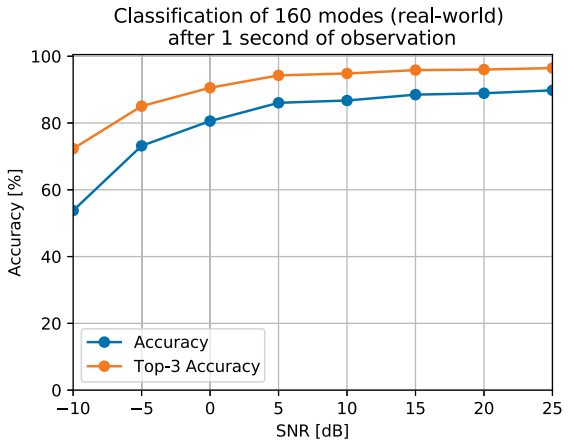

Figure 9 – Classification accuracy as average over all.

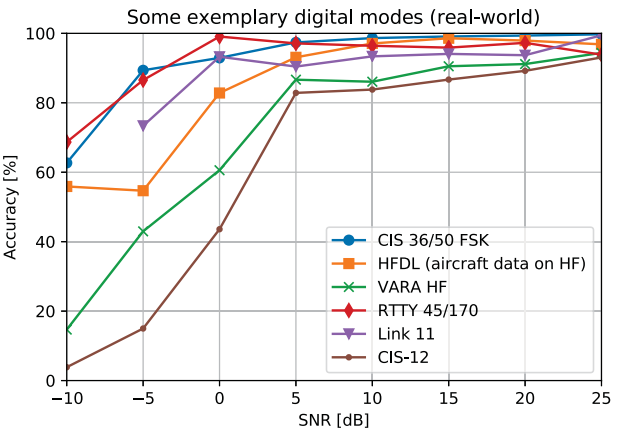

Figure 11 – Classification accuracy for some selected digital modes.

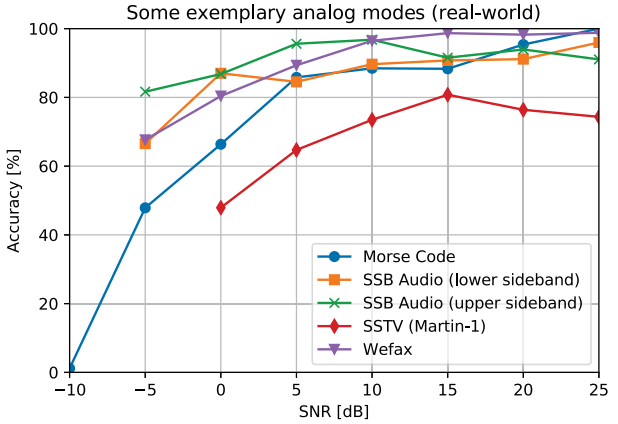

Figure 10 – Classification accuracy for some selected analog modes.

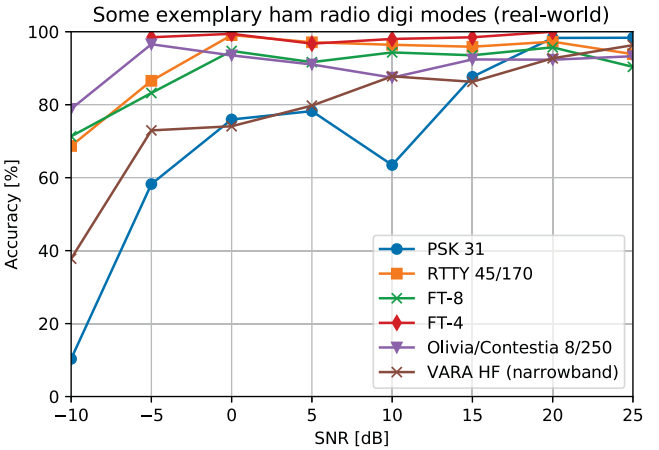

Figure 12 – Classification accuracy for some selected ham radio modes.

real-world signals are fed into the neural network in one second increments. The network then predicts the estimated signal class for each increment.

The accuracy measurement indicates the success rate of the classifier and ranges between 0 and 100% (accuracy = number of correct predictions / total number of predictions).

The top three accurate readings are reported. For the top three, the network outputs the three most likely classes. If one of these matches the true class, it is counted as correct.

The results for all modes are depicted in **Figure 9**. It shows particularly good accuracy values, which reach an average around 90% for high SNR values. This means that in 9 of 10 cases the classifier selected the correct mode out of 160 possible based on just one second of observation. The top three accuracy is approximately 95%. In addition, the classifier is robust to noise and achieves good accuracy also for low SNR signals.

Figures 10, 11, 12 show the results for a selection of some common shortwave signal types. Here, some variance over the different class types can be seen: While some modes may achieve accuracy below 80%, others are identified with almost 100% accuracy (at sufficiently large SNR values).

Although the neural network performs very well on practical signals, for some modes, the classification accuracy does not approach 100% even under high SNR conditions. There are several possible reasons for this, e.g., the comparably short observation time or the high similarity of some classes in the IQ domain can lead to confusion.

Summary and Outlook

Neural networks and machine learning are powerful tools for radio signal monitoring. The experiments described in this article show some of the potential of these new approaches for signal identification. Even for 160 modes, neural networks can provide decent classification results for real-world signals without the need for manually designed features for each mode. Since the application of machine learning is not restricted to pure signal identification, the approach can also be extended to related problems, like signal detection or joint classification and localization of signals in the spectrum.

Stefan Scholl received a German class A license, DC9ST, in 2006. He earned a diploma in electrical engineering in 2010, and PhD in 2018 from the University of Kaiserslautern, Germany. Having held several positions in industry and academia, his work has included forward error correction, FPGA implementations, signal processing, and AI for communication and radar applications. His interests include hardware and algorithms for software defined radio and shortwave communications.

Notes

[1] https://panoradio-sdr.de/the-world-of-shortwave-signals (2023)
[2] https://www.sigidwiki.com/wiki/Signal_Identification_Guide (2024)
[3] Roland Proesch: Technical Handbook for Radio Monitoring HF, 2019
[4] https://openai.com/chatgpt/
[5] Recommendation ITU-R F.1487: Testing of HF modems with bandwidths of up to about 12 kHz using ionospheric channel simulators, 2000


Statement of Ownership, Management and Circulation
(All Periodicals Publications Except Requester Publications)

Eric P. Nichols, KL7AJ
138 Shenandoah Dr., Fairbanks, AK 99712 | **kl7aj@arrl.net**

Self-Paced Essays—#30 Electronic Slide Rules

A look at how logarithmic methods evolved from manual tools to circuit-level implementations.

My first calculator was a slide rule. My dad made me learn how to use the thing when I was around nine years of age; he thought it would be great discipline. He wasn't wrong, but it took me a couple of decades to figure that out.

At El Camino College, back in 1972, (the year I was first licensed), Slide Rule was a required course for engineering majors. It was also the first year anyone was allowed to use calculators in any math class. I remember my slide rule instructor saying, "A calculator is a machine that will give you the wrong answer to fifteen decimal places." Great words of wisdom.

Because of a slide rule's inherent limitation of precision, one got particularly good at coming up with the *right answer,* even if that answer only had a decimal place or two. It was a great instrument for letting you separate the wheat from the chaff, so to speak.

Moving forward a few years, technologically, we come to the fully electronic version of the slide rule, the analog computer. Like the slide rule, the analog computer does most of its calculations (other than simple addition or subtraction) by the manipulation of logarithms. So, the heart of any full-function analog computer is the logarithmic amplifier, a device that's amazingly simple in concept, but a bit tricky to implement accurately. (**Figure 1**)

The two leftmost op-amps are logarithmic amplifiers, taking advantage of the logarithmic current vs voltage curve of a standard diode. These two amplifiers output the logarithm of the inputs, V1 and V2, respectively. The center op-amp is a summing amplifier, which, oddly enough, outputs the algebraic sum of the two input voltages. Finally, the last op-amp, with its preceding diode, forms an *antilog* amplifier. The output vb is the algebraic product of V1 and V2. This entire circuit does exactly what a slide rule does, performs multiplication by adding logarithms, but hopefully with a little more accuracy.

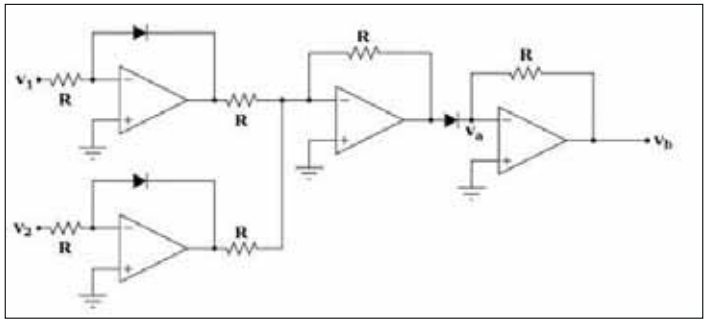

Figure 1 – Logarithmic amplifier circuit.

If we want to perform division, we would change the center op-amp from a summing amp to a differential amp, thus allowing us to subtract logarithms. (We still need to "de-logarithmize" the output of the summing amp in this case, as in the multiplier).

Now, the circuit has some serious limitations, primarily having a very low *dynamic range.* As it turns out, a diode has a very odd current to voltage transfer curve. It has a *continuously varying exponent*! This means, that, contrary to "popular opinion," the diode (of any kind) is only a *square law* device over an extremely narrow window. More practical log-amps use a transistor in the feedback loop, (or in the feed-forward path, in the case of the antilog amp) which greatly expands the square law region. Also, practical log-amps have temperature compensation circuitry since the exponent of a diode is highly temperature dependent. Although you can certainly build log-amps from discrete components, almost all modern log-amps are monolithic chips with all the bias and temperature compensation built in. As such, they are typically more expensive than your normal op-amps.

If you care to delve more into the math of diodes, here is the general Shockley diode equation:

$$I = I_s\left(\frac{V_D}{e^{nV_T}} - 1\right)$$

where,
I is the diode current,
I_S is the reverse-bias saturation current (or scale current),
V_D is the voltage across the diode,
n is the ideality factor, also known as the quality factor, emission coefficient, or the material constant,
V_T is the thermal voltage.

So, if you were to go about building a full-function analog computer, how would you go about doing that? Glad you asked

Figure 2 – MD 80 flight simulator.

because my friend Christopher Howard, KL1TL, did just that. But, perhaps more importantly, you might ask, *why* would anyone go about doing that? I believe we can learn more by answering the second question first.

Christopher maintains the MD-80 flight simulator (**Figure 2**) at Everts Air in Fairbanks, Alaska. There are a number of smaller simulators at the facility as well, but the MD-80 is the most elaborate, with full hydraulic articulation (in other words, it moves around and can make you airsick). It may be one of the most elaborate analog computers one will likely encounter in one's lifetime. At the heart of this beast is not only one analog computer, but arrays of them.

These take inputs from countless sensors around the simulator and apply visual and physical feedback, which allows the pilot or trainee to fly the machine as if it were the real thing. These calculations must be made *fast,* in real time, something the speediest digital supercomputers would be hard pressed to accomplish.

Now, not everything in the facility is analog. There are numerous "normal" computers that run "glue programs" to choreograph all the analog computers, but it's the analog computers that do all the close-to-the-hardware heavy lifting.

Rolling Your Own

Well, a few months ago, Christopher told me he wanted to build his own general purpose analog computer, just for self edification and education. Although he was highly skilled in running the "big stuff," he wanted to get right down to the basics.

Christopher paid several visits to my shack helping deplete my excess stash of banana cables and banana jacks, along with some relays and such, all to go toward his analog computer (**Figures 3** and **4**).

One of the most impressive things Christopher demonstrated with this "steampunk computer" was a beautifully synthesized damped oscillation. (I've described the damped oscillation in an earlier essay or two).

Now for the less ambitious experimenter, you can get this as a commercial kit form (**https://the-analog-thing.org/**). This

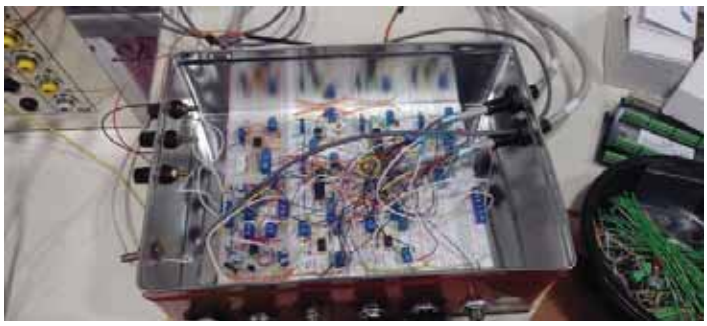

Figure 3 – Homebrew analog computer.

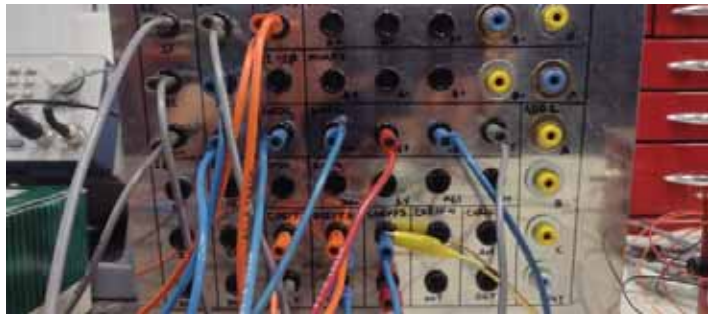

Figure 4 – Analog computer patch panel.

is produced by Anabrid GmbH (**Figure 5**), and is available for a few hundred dollars, U.S. As you can see, it uses a lot of patch cables, just like Christopher's entirely homebrew version.

Figure 5 – Anabrid analog computer.

Although discrete log amps are readily available, it is more common to buy them in the form of "multiplier" chips, which can be configured externally to form multiple math functions. Analog Devices (https://www.analog.com/en/product-category/analog-multipliers-dividers.html) is the acknowledged source for such devices.

I hope I've helped reinforce the idea that there's more than one way to skin a cat, and analog methods are powerful tools to have in our electronics arsenals.

Special thanks to Michael Heit, AD7VV, of Everts Air, for allowing me to wander around the simulator facility with minimal supervision, and Christopher Howard, KL1TL, for wobbling a few of my dormant brain follicles with this great project.
73! Eric.

DX Engineering Makes

Contest Season

Fun!

We make it easy to get what you need for higher scores: DX Engineering's RF-PRO-1B® Active Magnetic Loop Antenna and other receiving devices; HamPlus Antenna Switches; RigSelect's Pro Transceiver Switch and SO2R Controller; VA6AM, RF Meca, and 4O3A band pass filters; rigs like the Icom IC-7610; and more.

Contact us for the best products, fastest shipping, and most responsive service from experienced operators—a winning combination every time!

Make the Change to a More Satisfying Ham Radio Purchasing Experience

- Easy ordering by phone or web
- Products from over 180 leading manufacturers
- Friendly customer service from hams with a combined 1,000+ years in amateur radio
- Fastest shipping in the industry
- Responsive and ongoing technical support
- Not 100% happy? We make it right!

Order by Phone

800-777-0703 Country Code: +1
9 am to midnight ET, Monday-Friday
9 am to 5 pm ET, Weekends

Order Online

www.DXEngineering.com
Most orders over $99 ship free
Request a Free Catalog

Tech Support

330-572-3200
DXEngineering@DXEngineering.com
9 am to 7 pm ET, Monday-Friday
9 am to 5 pm ET, Saturday

DX 25™ ENGINEERING

bhi · HEIL HAM RADIO · INRAD international radio · PHONEMA · ve2dx ELECTRONICS DESIGN INC.

ON ALL BANDS

OnAllBands.com is dedicated to educating and informing the Amateur Radio community.

HANDBOOK 101

The Next Generation of Amateur Radio!

Softcover Book
Includes e-book.
Retail $69.95

Six-Volume Set
Includes e-book.
Retail $69.95

e-Book
Retail $69.95

Major Updates:

- Electromagnetic analysis and inexpensive tools for modeling circuits, antennas, and propagation.
- Higher-level modeling of transmitters and receivers.
- Preparing your station for emergency operations.
- Radio astronomy receiver and antenna design.
- Batteries and battery safety.
- NEC4 and antenna modeling software.
- SWR meters and related tests.
- RF safety and compliance with FCC exposure regulations.

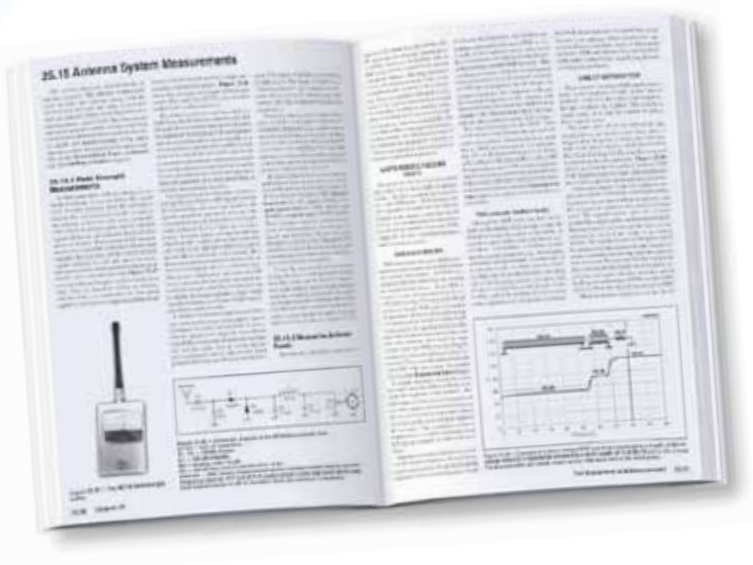

The ***ARRL Handbook*** is your complete guide to wireless technology experimentation, practice, and development. Since 1926, the ***Handbook*** has captured the state of radio science and technology in one authoritative work. Use it to delve into radio electronics, circuit design, digital modulation techniques, and equipment construction.

BONUS e-Book Download!

Your purchase includes the fully searchable digital edition of the printed book (PDF format), plus expanded content, software, PC board templates, and other support files.

Order online at www.arrl.org/shop | Call toll-free US 1-888-277-5289